TECHNICAL REPORT

ISO/TR 24679-5

First edition
2023-07

Fire safety engineering — Performance of structures in fire —

Part 5: Example of a timber building in Canada

Reference number
ISO/TR 24679-5:2023(E)

ISO copyright office
CP 401 • Ch. de Blandonnet 8
CH-1214 Vernier, Geneva
Phone: +41 22 749 01 11
Email: copyright@iso.org
Website: www.iso.org

Published in Switzerland

Contents

Page

Foreword

ISO (the International Organization for Standardization) is a worldwide federation of national standards bodies (ISO member bodies). The work of preparing International Standards is normally carried out through ISO technical committees. Each member body interested in a subject for which a technical committee has been established has the right to be represented on that committee. International organizations, governmental and non-governmental, in liaison with ISO, also take part in the work. ISO collaborates closely with the International Electrotechnical Commission (IEC) on all matters of electrotechnical standardization.

The procedures used to develop this document and those intended for its further maintenance are described in the ISO/IEC Directives, Part 1. In particular, the different approval criteria needed for the different types of ISO document should be noted. This document was drafted in accordance with the editorial rules of the ISO/IEC Directives, Part 2 (see www.iso.org/directives).

ISO draws attention to the possibility that the implementation of this document may involve the use of (a) patent(s). ISO takes no position concerning the evidence, validity or applicability of any claimed patent rights in respect thereof. As of the date of publication of this document, ISO had not received notice of (a) patent(s) which may be required to implement this document. However, implementers are cautioned that this may not represent the latest information, which may be obtained from the patent database available at www.iso.org/patents. ISO shall not be held responsible for identifying any or all such patent rights.

Any trade name used in this document is information given for the convenience of users and does not constitute an endorsement.

For an explanation of the voluntary nature of standards, the meaning of ISO specific terms and expressions related to conformity assessment, as well as information about ISO's adherence to the World Trade Organization (WTO) principles in the Technical Barriers to Trade (TBT), see www.iso.org/iso/foreword.html.

This document was prepared by Technical Committee ISO/TC 92, *Fire safety*, Subcommittee SC 4, *Fire safety engineering*.

A list of all parts in the ISO 24679 series can be found on the ISO website.

Any feedback or questions on this document should be directed to the user's national standards body. A complete listing of these bodies can be found at www.iso.org/members.html.

Introduction

This document provides an example of the application of ISO 24679-1. The procedure described in this document is intended to follow the principles outlined in ISO 24679-1. It therefore preserves the numbering of subclauses in ISO 24679-1, omitting numbered subclauses for which there is no text or information relevant to this example.

The example provided in this document is intended to illustrate the implementation of the steps of fire resistance assessment, as defined in ISO 24679-1, and to demonstrate how ISO 24679-1 can be applied to different building regulatory systems. It is not intended to demonstrate full conformance of a performance-based fire engineering design seeking approval. Therefore, only a limited number of fire design scenarios and structural assessments are presented.

Fire safety engineering — Performance of structures in fire —

Part 5:
Example of a timber building in Canada

1 Scope

This document provides a fire engineering application relative to the fire resistance assessment of a multi-storey timber building according to the methodology given in ISO 24679-1. In an attempt to facilitate the understanding of the design process presented herein, this document follows the same step-by-step procedure as that given in ISO 24679-1.

The fire safety engineering approach is applied to a multi-storey timber building with respect to fire resistance and considers specific design fire scenarios, which impact the fire resistance of structural members.

A component-level (member analysis) approach to fire performance analysis is adopted in this worked example. Such an approach generally provides a more conservative design than a system-level (global structural) analysis or an analysis of parts of the structure where interaction between components can be assessed. An advantage of the component-level approach is that calculations can be done with the use of simple analytical models or spreadsheets. Advanced modelling using computational fluid dynamics is presented to replicate an actual office cubicle fire scenario and for assessing timber contribution to fire growth, intensity and duration, if any. The thermo-structural behaviour of the timber elements is assessed through advanced modelling using the finite element method.

The fire design scenarios chosen in this document are only used for the evaluation of the structural fire resistance. They are not applicable for assessing, for example, smoke production, tenability conditions or other life safety conditions.

2 Normative references

The following documents are referred to in the text in such a way that some or all of their content constitutes requirements of this document. For dated references, only the edition cited applies. For undated references, the latest edition of the referenced document (including any amendments) applies.

ISO 13943, *Fire safety — Vocabulary*

ISO 23932-1, *Fire safety engineering — General principles — Part 1: General*

ISO 24679-1, *Fire safety engineering — Performance of structures in fire — Part 1: General*

3 Terms and definitions

For the purposes of this document, the terms and definitions given in ISO 13943, ISO 23932-1 and ISO 24679-1 apply.

ISO and IEC maintain terminology databases for use in standardization at the following addresses:

— ISO Online browsing platform: available at https://www.iso.org/obp

— IEC Electropedia: available at https://www.electropedia.org/

4 Design strategy for fire safety of structures

4.1 General design process for fire safety of structures

The built environment used in this example is a medium-rise office building. To accommodate tenant office functions, the building is separated into multiple compartments by floors and walls. Given that an office space typically consists of several office workstation or cubicles, it is likely that a fire will spread to neighbouring elements and eventually across the entire floor surface. As such, a fully-developed compartment fire is expected in each office suite of the building.

The structural elements are of glue-laminated timber beams and columns, where portions of the primary structural timber elements are left exposed for aesthetic purposes. The secondary structural elements are protected against fire using fire-resistance rated gypsum boards.

The fire development was studied using computational fluid dynamics (CFD) modelling, with specific considerations for capturing the potential fuel contribution from the structural timber elements. Time-temperature curves were produced, as well as relevant key events during the fire development (growth, flashover conditions, consumed fuel load, etc.).

Simplified and advanced models have been used to define the thermal actions applied to the timber elements. The thermomechanical behaviour of the main structure of the office building, based on simplified and advanced methods, is carried out as a function of the actual thermal actions defined previously.

4.2 Practical design process for fire safety of structures

Refer to ISO 24679-1 for more information about the various steps and parameters to be considered when assessing the behaviour of structures subjected to fire exposure.

5 Quantification of the performance of structures in fire

5.1 Step 1: Scope of the project for fire safety of structures

5.1.1 Built-environment characteristics

The built environment consists of a 6-storey office building constructed with a timber structure. The floor area of each storey is approximately 960 m^2 for a total floor area of 5 760 m^2. Access to each floor is provided by two reinforced concrete exit stairs located at each end of a public corridor. An elevator shaft made of reinforced concrete is also provided and is located near the centre of the floor area. Figure 1 illustrates the structural framing of the building. Every floor has a clear interior floor/ceiling height of 3,0 m. These floor assemblies are required to form a fire separation with a fire-resistance rating not less than 1 hour. Load-bearing walls and columns are required to provide a fire-resistance rating not less than that required for the supported elements and assemblies.

According to the applicable national prescriptive provisions,[4] a 6-storey office building using a timber structural system is required to be fully protected by an automatic sprinkler system conforming to NFPA 13.[5] It is also required to have fire detection and fire alarm systems.

The primary and secondary structural elements consist of glued-laminated timber beams and columns of the 20f-E and 12c-E Spruce-Pine (SP) stress grades.[6],[7] The floor structure is made of traditional visually-graded solid-sawn double tongue-and-groove plank decking, of the Spruce-Pine-Fir (SPF) No.2 visually-graded lumber grade.[8] The plank decking is laid perpendicularly to the supporting secondary beams, which are spaced every 2 m (centre to centre). All timber elements conform to the national lumber grading rules.[9] The structural engineering design, for ambient/normal conditions, conforms to the relevant design standard.[8]

Concealed connections between the primary and secondary structural elements are used, in which metallic components such as self-tapping screws driven at 45° are fully embedded into the wood

members to limit potential thermo-mechanical degradation from fire exposure. Figure 2 illustrates the floor structure and location of load-bearing elements. Figure 3 illustrates the connections and their embedment into the load-bearing elements. The characteristics of the load-bearing elements assumed in this example are given in Table 1. The dimensions of the main elements are greater than required for structural purposes due to the embedment of the load-bearing elements; they need to be able to provide sufficient bearing lengths to the embedded main and secondary beams. The chosen elements considered for demonstrating the procedure of ISO 24679-1 are a main beam, B1, located above the fire source and its supporting column, C2, towards the exterior wall.

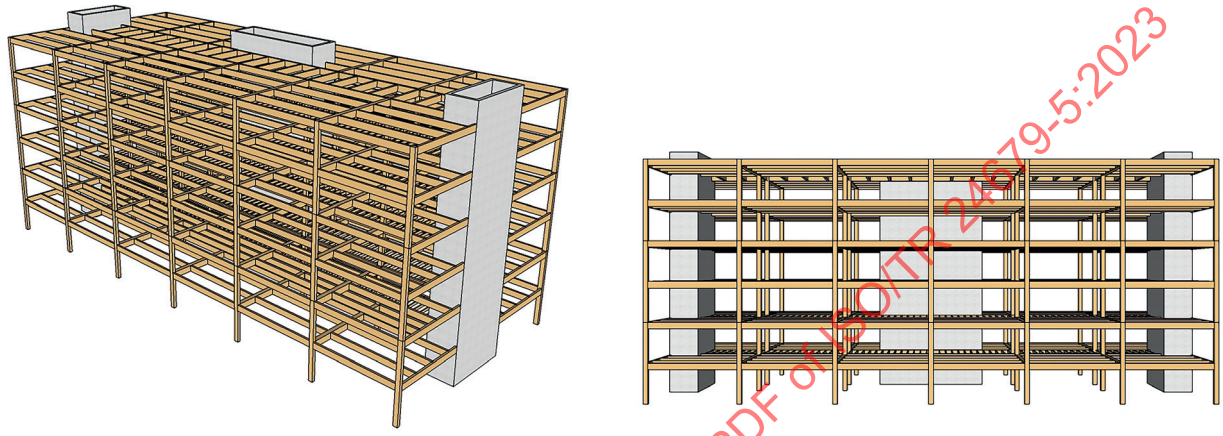

a) Isometric view **b) Front view**

Figure 1 — Structural frame

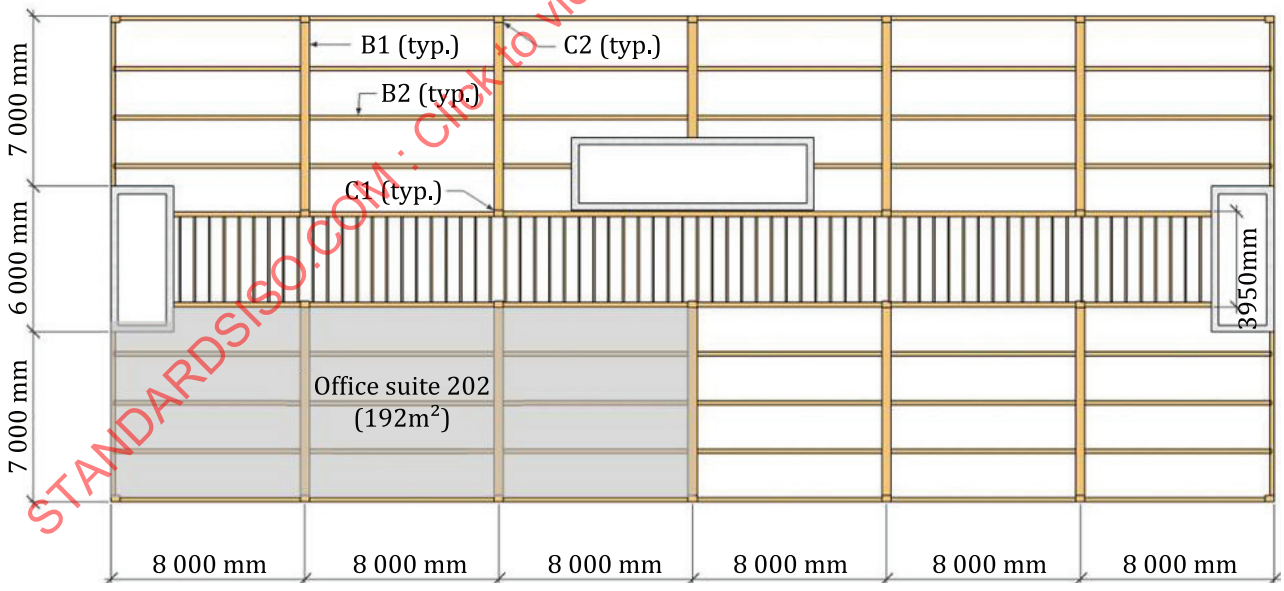

Figure 2 — Typical floor structural configuration

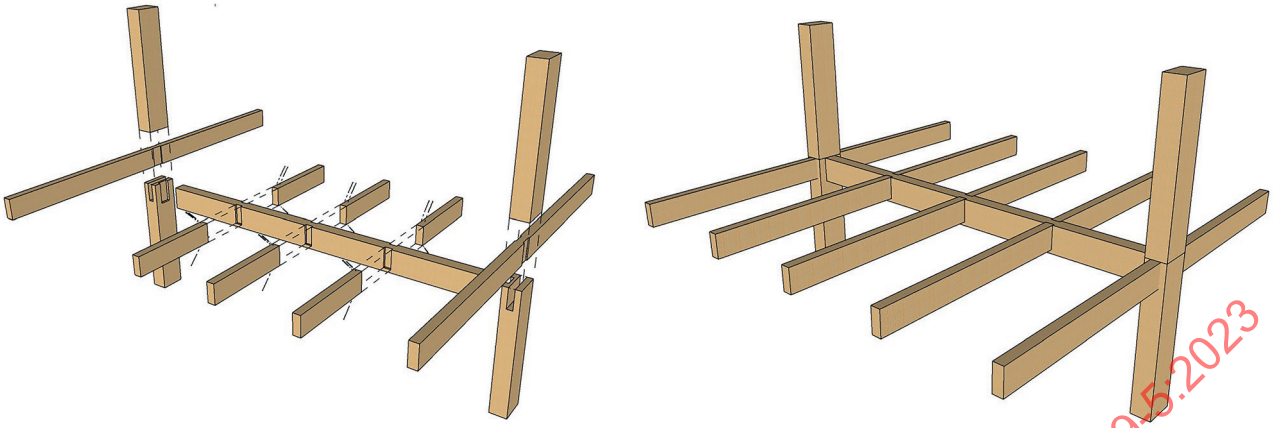

a) "Before" frame assembly **b) "After" frame assembly**

Figure 3 — Detailing of the connections

Table 1 — Load-bearing elements characteristics — Preliminary design (ambient conditions)

Element	Type	Dimensions mm	Gypsum board
B1	Glulam 20f-E	265 × 532[a]	None
B2	Glulam 20f-E	175 × 456[b]	None
C1	Glulam 12c-E	418 × 365	None
C2	Glulam 12c-E	342 × 365	None
Decking	S-P-F No.2	89 × 133	1 × 16 mm Type X
Partitions	Wood studs	38 × 89[c]	2 × 13 mm Type X

[a] At 8 000 mm centre-to-centre (c/c).

[b] At 2 000 mm c/c.

[c] At 600 mm c/c.

The dropped-ceiling assembly forms a cavity filled with non-combustible insulation for providing the required sound transmission class (Figure 4). The exposed ceiling consists of a single layer of 16 mm fire-rated gypsum board (e.g. Type X) fastened to the secondary beams in conformance with national specifications.[10],[11] With this specific configuration, a limited portion of the primary beams and columns are left exposed and can thus contribute to fire growth and severity.

Partitions made from wood stud walls are used to separate the office suites and the public corridor within the floor area. They are constructed using 38 mm × 89 mm wood studs spaced at 600 mm. Two (2) layers of 13 mm Type X gypsum board (i.e. fire-resistance rated gypsum boards) are installed on both sides of the studs, providing a 1 hour fire-resistance rating when tested by a standard fire-resistance test.[12] The inside cavities of the stud walls are filled with 89-mm thick non-combustible insulation in order to provide both the prescribed fire-resistance rating and the sound transmission class.

According to the applicable national prescriptive provisions, these partitions are not required to be constructed as a fire separation and are not required to provide a fire-resistance rating because the building is entirely protected by automatic sprinklers and the maximum travel distance from any part of the floor area to an exit is not more than 45 m. Assessment of the fire performance of the partitions is therefore beyond the scope of this document.

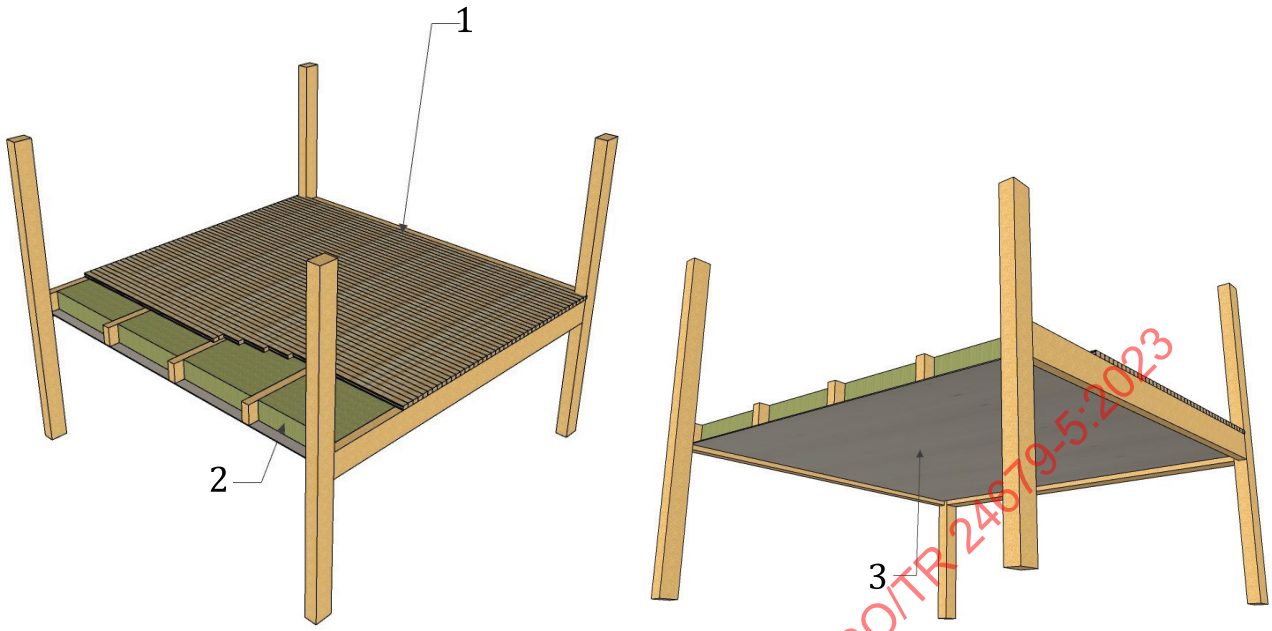

a) Isometric view **b) View of the ceiling**

Key

1 89 mm × 133 mm plank decking with double tongue-and-groove

2 concealed spaces filled with non-combustible insulation

3 16 mm type X gypsum board

Figure 4 — Floor assembly

For the purpose of this document, the office suite to be analysed is located on the second floor and represents the compartment of fire origin. It is a 192 m^2 open-space office suite in which cubicles with computers, desks, chairs and filing cabinets are uniformly distributed across the floor area (Figure 5).

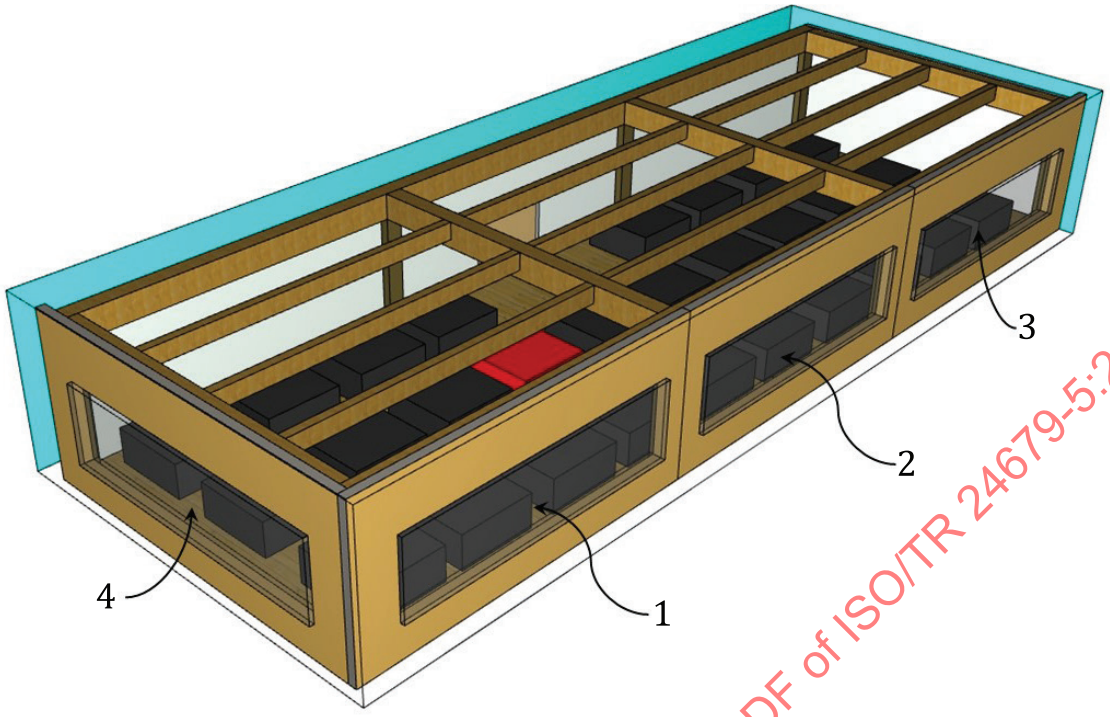

Key

1 window 1
2 window 2
3 window 3
4 window 4

Figure 5 — Isometric view of office suite (compartment of fire origin)

5.1.2 Fuel loads

Fire loads consist of the total energy content of combustible materials in a building, a space or an area including furnishing and contents within a compartment (i.e. moveable fire load) and combustible materials used as structural elements, interior finishes or installed in concealed spaces (i.e. fixed fire load). The office suite where the fire is assumed to start consists of an open-space configuration with 28 cubicles and an engineered hardwood flooring of 13 mm in thickness, see Figure 5. Each cubicle measures 1,8 m × 1,8 m (3,24 m^2). The typical combustible materials found in cubicles are paper, wood, plastic and textiles.

An average moveable fuel load density of 420 MJ/m^2 is typically assigned for an office space.[13-15] However, it is typically recommended to use the 95th percentile value for fire design purposes. A 95th percentile value of 760 MJ/m^2 is suggested for offices in Reference [14]. Zalok[16] found 95th percentile fuel loads of 8 822 MJ and 15 666 MJ for small floor area cubicle offices (11 m^2) and large floor area enclosed offices (25 m^2), respectively. It was also reported that offices with large floor area result in lower fire load densities (626 MJ/m^2), when compared to that of smaller floor areas (802 MJ/m^2). Given the large floor area of this example (192 m^2), a value of 735 MJ/m^2 is deemed appropriate, and consistent with that provided in References [14-16].

The National Institute of Standards and Technology (NIST)[17] evaluated the heat release rate (HRR) of a single workstation covering a floor area of 1,93 m × 1,63 m (3,15 m^2) as well as multiple workstations (4 workstations assembled in similar manner as the single workstation). A total fuel load mass of 273,2 kg was measured for the single workstation. Assuming an effective heat of combustion

of 18 MJ/kg, a total energy of 4 917 MJ is estimated for a single workstation. The HRR obtained in the NIST study is illustrated in Figure 6 a). The workstation HRR development curve used for performing the computational fluid dynamics (CFD) modelling in Fire Dynamics Simulator (FDS) version 6.7 is shown in Figure 6 b). The workstation HRR development curve is further explained below.

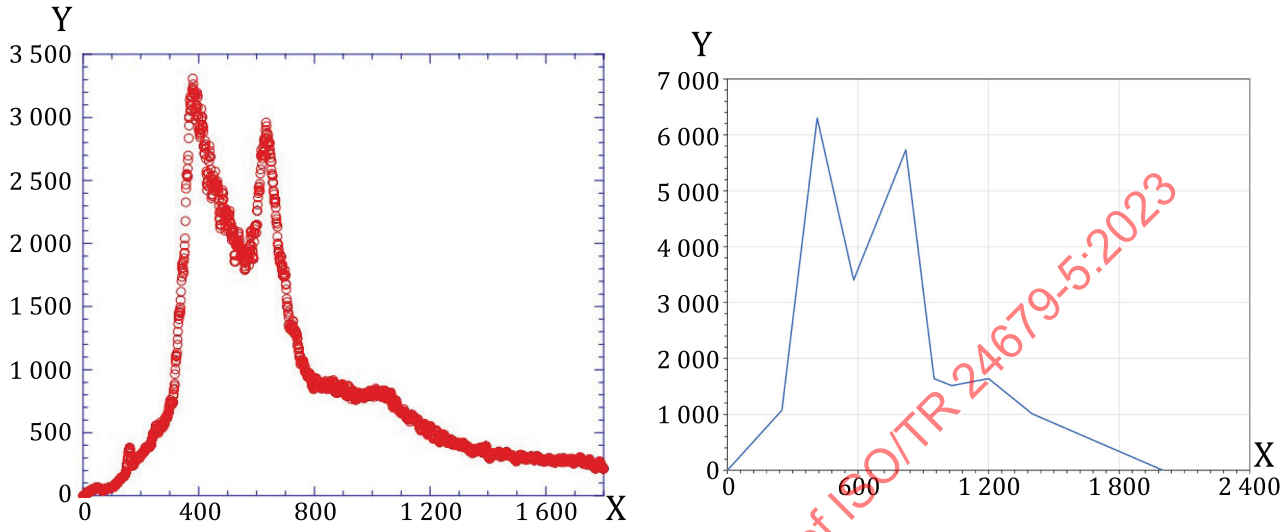

a) HRR, as presented in Reference [17]

b) HRR implemented in FDS

Key

X time (s)

Y heat release rate (kW)

Figure 6 — Heat release rate of a single workstation

For the purpose of this document, the moveable fuel load energy density, *FLED,* is comprised of a total of 28 cubicles uniformly distributed along the 192 m^2 floor area, $FLED_{cubicles}$, and the hardwood flooring, $FLED_{flooring}$. In an attempt to replicate a uniform fuel load density of 735 MJ/m^2, each cubicle has been set to 4 082 MJ. The cubicle individual HRR development growth has been kept similar to that shown in Figure 6 b). The 13-mm thick hardwood flooring density is assumed to be 600 kg/m^3 with an effective heat of combustion of 18 MJ/kg. A resulting moveable FLED value of 735 MJ/m^2 is obtained using Formula (1).

$$FLED = FLED_{flooring} + FLED_{cubicles} \quad (1)$$

The total fuel mass, m_{Total}, can be estimated from the fire load energy density (*FLED*), the total floor area, A_f, of 192 m^2, and an effective heat of combustion, H_{eff}, of 18 MJ/kg (wood equivalent), using Formula (2):

$$m_{Total} = \frac{A_f \cdot FLED}{H_{eff}} \quad (2)$$

The total fuel mass of 7 840 kg is required for determining the design fire curve, as presented in 5.4.2.

The moveable fuel load density calculated in Formula (2) does not include the potential contribution from the timber structural elements. The latter will be explicitly considered when performing CFD modelling, as described in 5.4.3.3.

5.1.3 Mechanical actions

According to the applicable national design requirements,[18] the load combination, *P,* for a rare/accidental event such as a fire is taken as shown in Formula (3):

$$P = 1{,}0\ D + (\alpha L + 0{,}25\ S) \tag{3}$$

where

D is the permanent load;

α is taken as 1,0 for storage areas, equipment areas and service rooms, or 0,5 for other occupancies;

L is the live load due to occupancy;

S is the snow load.

For an office space, a minimum live load of 2,4 kPa is prescribed in the national design provisions.[18]

Given that the low probability that all floors of a multi-storey building would be structurally loaded to its full live load simultaneously, a live load reduction factor can be used based on the tributary area supported by columns. For a column supporting a tributary area greater than 20 m^2 and for this type of building occupancy, as with the case of column C2 (32 m^2) in this office building, the applicable national design requirements[18] allow the applied live load to be multiplied by the value shown in Formula (4):

$$0{,}3 + \sqrt{\frac{9{,}8}{B}} \tag{4}$$

where B is the tributary area of the supporting column (m^2).

While post-earthquake fires can occur, fires and earthquakes are both considered as rare events and thus deemed not to occur at the same time. Therefore, horizontal actions due to wind and seismic forces are typically not considered for structural fire-resistance, unless specifically stipulated in the applicable building code.

5.2 Step 2: Identifying objectives, functional requirements and performance criteria for fire safety of structures

5.2.1 Objectives and functional requirements for fire safety of structures

Conducting a rational fire safety design of structures requires the establishment of fire safety objectives and functional requirements. With respect to fire resistance of structures, the qualitative objectives typically relate to the fire safety of occupants as well as the fire protection of the building.

From the applicable national building code, the objective for fire safety is to limit the probability that, as a result of the design, construction or demolition of the building, a person in or adjacent to the building will be exposed to an unacceptable risk of injury due to fire caused by:

a) a fire impacting areas beyond its point of origin; and

b) collapse of physical elements due to a fire.

Similarly, the objective for fire protection of the building is to limit the probability that, as a result of the design, construction or demolition of the building, the building or adjacent buildings will be exposed to an unacceptable risk of damage due to fire caused by:

a) a fire impacting areas beyond its point of origin; and

b) collapse of physical elements due to a fire.

In addition to these objectives, functional requirements are typically provided and linked to the objectives to clarify the intent. With respect to structural fire resistance, the functional requirements (also called functional statements in the applicable national building code) are to retard the effects of a fire on areas beyond its point of origin and the retard failure or collapse due to effects of the fire. The pairing of the functional statements and the objectives results in the following statements of intent:

a) to limit the probability that materials, assemblies or structural members will have insufficient resistance to the spread of fire, which could lead to harm to persons;

b) to limit the probability that materials, assemblies or structural members will have insufficient resistance to fire, which could lead to their failure or collapse, which could lead to harm to persons;

c) to limit the probability that materials, assemblies or structural members will have insufficient resistance to the spread of fire, which could lead to damage to the building; and

d) to limit the probability that materials, assemblies or structural members will have insufficient resistance to fire, which could lead to their failure or collapse, which could lead to damage to the building.

In satisfying the functional requirements, it is essential to take into consideration the existence of active and passive fire control systems and their effectiveness.

5.2.2 Performance criteria for fire safety of structures

Performance criteria are used to determine whether the objectives and functional requirements for the fire safety of structures have been satisfied.

It is stipulated in a national design standard that structures are to be designed to prevent collapse of the structure itself and to exhibit adequate load-bearing capacity and capability to maintain structural integrity for a sufficient time.[19] According to Reference [19], ensuring structural integrity for complete burn out of the moveable fire load of any fire compartment is only required for tall (high) buildings. In the context of this worked example, a 6-storey office building does not classify as a tall (high) building, as defined in the applicable national prescriptive provisions, and is therefore not required to achieve complete burnout of the moveable fuel content.

Therefore, the performance criterion used in this worked example is taken as the time at which the impinging heat flux on the exposed surfaces of the timber elements reduces below 5 kW/m^2. Below this threshold, it is assumed that the moveable fuel load will most likely be consumed and that smouldering timber elements will stop charring and no longer contribute to the fire heat release rate.[20] A reduction in the net emitted energy to the exposed timber surfaces results in a reduction in the mass production of volatiles, which will result in extinction if such reduction is sufficient (i.e. flaming will cease at the timber surfaces). Moreover, auto-extinction of flaming combustion of Spruce with a density of 425 kg/m^3 has been found to occur if the timber mass loss rate reduces below 3,93 g/m^2·s and the heat flux is less than 43,6 kW/m^2.[21,22] This threshold has been found to be dependent upon the timber species, but not the density[22].

The objectives and functional requirements are deemed to be satisfied when the load-bearing function, and separating function where appropriate, remain fulfilled until the criteria of heat flux and mass loss rate are reached. The proposed performance criteria are considered as reasonable assumptions based on scientific knowledge available at the time of writing this document. Other performance criteria could be used as new evidence is made available, provided they are supported by technical test data.

5.2.2.1 Performance criteria to limit fire spread (compartmentation)

The compartmentation of a built environment in order to prevent or to limit the fire spread can be achieved by load-bearing elements such as walls and floors, or by non-load-bearing elements, such as partition walls, doors, windows, etc. These elements need to satisfy functional requirements related to integrity, insulation and mechanical resistance or stability.

Separating elements used to compartment a building are required to achieve the following two performance criteria, as found in ISO 834-1.

— Insulation criteria: the assembly is required to prevent the rise in temperature of the unexposed side of separating (load-bearing and non-load-bearing) elements from being greater than 180 °C at any location, or an average of 140 °C, above the initial temperature.

— Integrity criteria: the assembly is required to prevent the passage of flame or gases hot enough to ignite a cotton pad or through gaps formed through separating (load-bearing and non-load-bearing) elements.

The performance criterion is that no spread of fire occurs beyond the compartment of fire origin, until both the impinging heat flux on the exposed surfaces of the timber elements and mass loss rate reduce below the thresholds cited in 5.2.2. The insulation and integrity criteria are to be fulfilled for this entire period of time. The performance criteria provided herein are assumed to be acceptable, based on scientific data and engineering principles. Other performance criteria can potentially be used, provided they are supported by technical test data.

5.2.2.2 Performance criteria to limit structural damage (structural stability)

Load-bearing elements used in a building are required to achieve the following performance criterion, as found in ISO 834-1.

— Load-bearing criterion: the load-bearing elements used to provide the structural stability are required to maintain the applied loads during the complete duration of the fire including the decay phase, or a specified period of time.

Even in the absence of collapse, deformation can still affect exit paths, endangering life safety, and can cause considerable property damage. As such, prevention of collapse and/or limitation of deformation are essential for load-bearing structural members and for load-bearing barriers, which also provide fire containment.

The performance criterion is that no excessive deflection and no structural collapse of any load-bearing element will occur until both the impinging heat flux on the exposed surfaces of the timber elements and mass loss rate reduce below the thresholds cited 5.2.2. The performance criteria provided herein are assumed to be acceptable, based on scientific data and engineering principles. Other performance criteria can potenially be used, provided they are supported by technical test data.

5.3 Step 3: Trial design plan for fire safety of structures

The trial design plan for fire safety of structures is an elaboration of the strategy for fire safety of structures and consists of a set of design elements for the fire safety of structures, such as stability and compartmentation. For the purpose of this document, a preliminary design was carried out in normal (room) conditions to determine the dimensions of the various structural timber components, as presented in Table 1.

Should the fire safety objectives stated in 5.2 be inconclusive using these preliminary dimensions, an iterative design process is to be undertaken to determine suitable dimensions of the timber elements that will fulfil the load-bearing function at both ambient and fire conditions.

5.4 Step 4: Design fire scenarios and design fires (thermal actions)

5.4.1 General

Design fire scenarios and design fires are an important step in the assessment of the performance of structures in fire. It is noted that a design fire scenario is a specific qualitative description of the development of a fire whereas a design fire (thermal actions) is a quantitative description of assumed fire characteristics within a design fire scenario.

5.4.2 Design fire scenarios

Figure 7 shows the event tree of 4 fire scenarios for office buildings.[23] It can be observed that the scenario where sprinklers do not activate and where fire department response is 20 min has the lowest probability of occurrence (P = 0,011). However, this design fire scenario would become more challenging for a structural frame within a relatively small compartment if the fire were to become fully-developed. The most likely scenario to occur is when sprinklers activate and the fire department responds rapidly (P = 0,801). These scenarios are selected for further analysis.

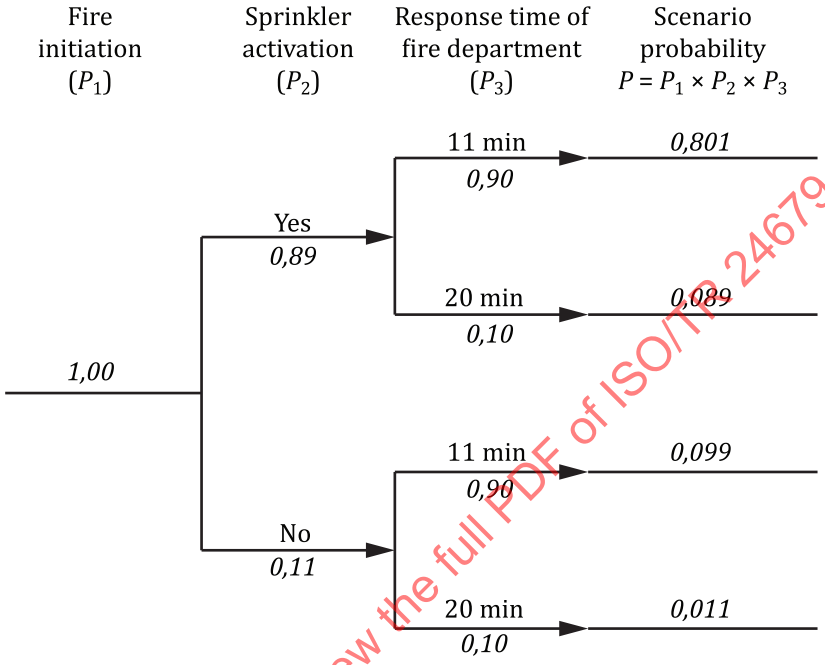

where:

P is the scenario probability;

P_1 is the fire initiation probability;

P_2 is the sprinkler activation probability;

P_3 is the response time of the fire probability.

Figure 7 — Event tree of an office building, as presented in Reference [23]

The following four scenarios are chosen for analysis in the present example. Some rationale for the selection is also provided for each scenario.

1) **Scenario 1**: HRR development of medium and fast t^2-fires assuming the maximum ventilation factors (glass from all windows is assumed to be open/broken) in which fuel contribution from structural timber elements and the effects of sprinkler activation on fire growth and the response of the fire department are ignored. This scenario would represent the comparison basis for verifying that the assumptions and parameters used in the CFD modelling are sufficiently conservative.

2) **Scenario 2**: fully-developed fire in which fuel contribution from structural timber elements and the effects from sprinkler activation on fire growth and the response of the fire department are ignored. This scenario represents the comparison basis for verifying and quantifying timber contribution to fire growth, intensity and duration using a CFD modelling.

3) **Scenario 3**: fully-developed fire in which fuel contribution from structural timber elements is considered, but the effects of sprinkler activation on fire growth and the response of the fire

department are ignored. The results from the CFD modelling of this scenario are compared to that of the CFD modelling of scenario 2.

4) **Scenario 4**: same as scenario 3, but with consideration of the effects of sprinkler activation on fire growth but without the fire department response.

The floor configuration overlooked in this document results in having the cubicle of fire origin located directly beneath the mid-span of a timber beam to facilitate ignition of that beam. However, as previously indicated, this document is not intended to demonstrate full conformance of a performance-based fire engineering design seeking approval. Therefore, only a limited number of fire design scenarios are being presented and evaluated to demonstrate how the design process given in ISO 24679-1 can be applied in this situation. However, in a design that will be submitted to the authorities for approval, multiple scenarios are to be considered by the designers.

5.4.3 Design fires (thermal actions)

As mentioned in ISO 24679-1, actions for consideration when assessing the behaviour of a structure in fire include thermal actions or design fires from realistic fire scenarios. Typically, thermal actions or design fires are given either as time-temperature relationships or as time-heat flux relationships. When estimating the temperature or heat flux effects on separating and structural elements, both convective and radiative heat effects are to be considered.

In this example, design fires are determined using simple analytical formulae and numerical calculations from computational fluid dynamics (CFD) modelling. Scenario 1 serves in determining a simple representation of an office fire using t^2-fires. Scenario 2 is produced using CFD modelling without consideration of timber elements contributing to fire growth and intensity and without any intervention from fire fighters or automatic sprinklers. The results are compared to those of scenario 1, namely with respect to growth rate, flashover conditions, ventilation conditions and heat release rate. Scenario 3 is the same as scenario 2, but with consideration of timber elements when they reached critical conditions for ignition and combustion. Scenario 4 is only used to demonstrate the effectiveness of automatic sprinklers on fire growth and heat release rate.

5.4.3.1 Design fire for scenario 1 (t^2-fire)

A design fire typically includes an incipient phase characterized by a number of sources, a growth phase ranging from fire propagation to flashover conditions, a fully-developed phase characterized by a steady burning rate based on ventilation conditions, a decay phase where fire severity declines and lastly the extinction where no more energy is produced. Events such as automatic sprinkler activation and window glass breakage will influence the development and growth of a given design fire scenario.

As detailed in ISO/TS 16733-2, the maximum heat release rate following flashover of a design scenario can be taken as the lesser of the ventilation-controlled and fuel-controlled heat release rates, $\dot{Q}_{\mathrm{v}}$ and $\dot{Q}_{fuel}$ respectively. The maximum ventilation-controlled heat release rate can be estimated using Formula (5).

$$\dot{Q}_{\mathrm{v}} = 1\,500\, A_{\mathrm{V}} \sqrt{H_{\mathrm{V}}} \tag{5}$$

where

A_{V} is the sum of the area of all openings, in m^2;

H_{V} is the average height of openings, in m.

The compartment has 4 openings, 6,7 m in width by 1,8 m in height, for a total area, A_{V}, of 48,24 m^2. All windows are the same dimensions. The average height, H_{V}, is taken as 1,8 m, resulting in a maximum ventilation-controlled heat release rate of 97 MW.

As presented in ISO/TS 16733-2, an office building can be modelled using a medium growth t^2-fire, α taken as 0,012 kW/s^2. The growth period, τ_{growth}, is then calculated as 2 844 s (47,4 min), according to Formula (6):

$$\tau_{growth} = \sqrt{\dot{Q}_{max} / \alpha} \tag{6}$$

During the growth phase, a mass of burned fuel, m_{growth}, of 5 114 kg is determined according to Formula (7):

$$m_{growth} = \frac{\int_{\tau_0}^{\tau_{growth}} \dot{Q} d\tau}{H_{eff}} = \frac{\alpha \tau_{growth}^3}{3 H_{eff}} \tag{7}$$

It is typically assumed that 80 % of the remaining fuel at the start of the steady-state period is pyrolized during this period. As such, the duration of the steady-state period, τ_{steady}, is taken as 404 s (6,7 min), calculated according to Formula (8):

$$\tau_{steady} = \frac{0,8\left(m_{total} - m_{growth}\right)}{\dot{Q}_{max} / H_{eff}} \tag{8}$$

A conservative assumption is to consider that the decay follows a linear relationship until full burn-out of the fuel content. The decay phase is initiated after 54,1 min ($\tau_{growth} + \tau_{steady}$), and its duration, τ_{decay}, is calculated as 202 s (3,4 min), using Formula (9):

$$\tau_{decay} = \frac{0,4\left(m_{total} - m_{growth}\right)}{\dot{Q}_{max} / H_{eff}} \tag{9}$$

The total duration of this design fire, τ_{fire}, is 57,5 min, taken as the sum of the growth, steady-state and decay periods according to Formula (10).

$$\tau_{fire} = \tau_{growth} + \tau_{steady} + \tau_{decay} \tag{10}$$

An additional t^2 design fire using a fast growth rate was also modelled and intended to replicate the potential contribution of the timber elements to fire growth, intensity and duration. The key characteristics for both medium and fast t^2 fires are given in Table 2 and the resulting design fire curves are shown in Figure 8. A discussion with respect to these t^2-fires compared to CFD modelling is given in 5.4.3.2 and 5.4.3.3.

Furthermore, when windows can become a part of the ventilation areas (openings) as a function of time (e.g. due to glass breakage from heat or extreme pressure), it is recommended to conduct a sensitivity analysis where both a high and low percentage of broken windows is assumed. Figure 9 shows the HRR from the 4 different ventilation factors provided by the opening of 1, 2, 3 and 4 windows and a medium t^2-fire. It can be observed that the scenario in which all 4 windows are opened/broken provides the most severe fire in terms of maximum heat release rate. The scenario in which only 1 window is opened/broken presents the longer fire duration. The maximum heat release rates are estimated as 24,3 MW, 48,5 MW, 72,8 MW and 97,1 MW for the scenarios having 1, 2, 3 and 4 windows opened, respectively. For the case of 1 window open, it is thought unlikely that the heat release rate would be sufficient to significantly challenge the timber structural elements.

Further details on other factors to be considered are provided in 5.9.

Table 2 — t^2 fires characteristics

Characteristic	Medium t^2 (α = 0,012 kW/s^2)	Fast t^2 (α = 0,047 kW/s^2)
Growth period		
τ_{growth}	47,4 min	24,0 min
m_{growth}	5 114 kg	2 584 kg
Steady-state period		
τ_{steady}	6,7 min	13,0 min
m_{steady}	2 181 kg	4 205 kg
Decay period		
τ_{decay}	3,4 min	6,5 min
m_{decay}	545 kg	1 051 kg
Total duration		
τ_{Total}	57,5 min	43,5 min
m_{Total}	7 840 kg	7 840 kg

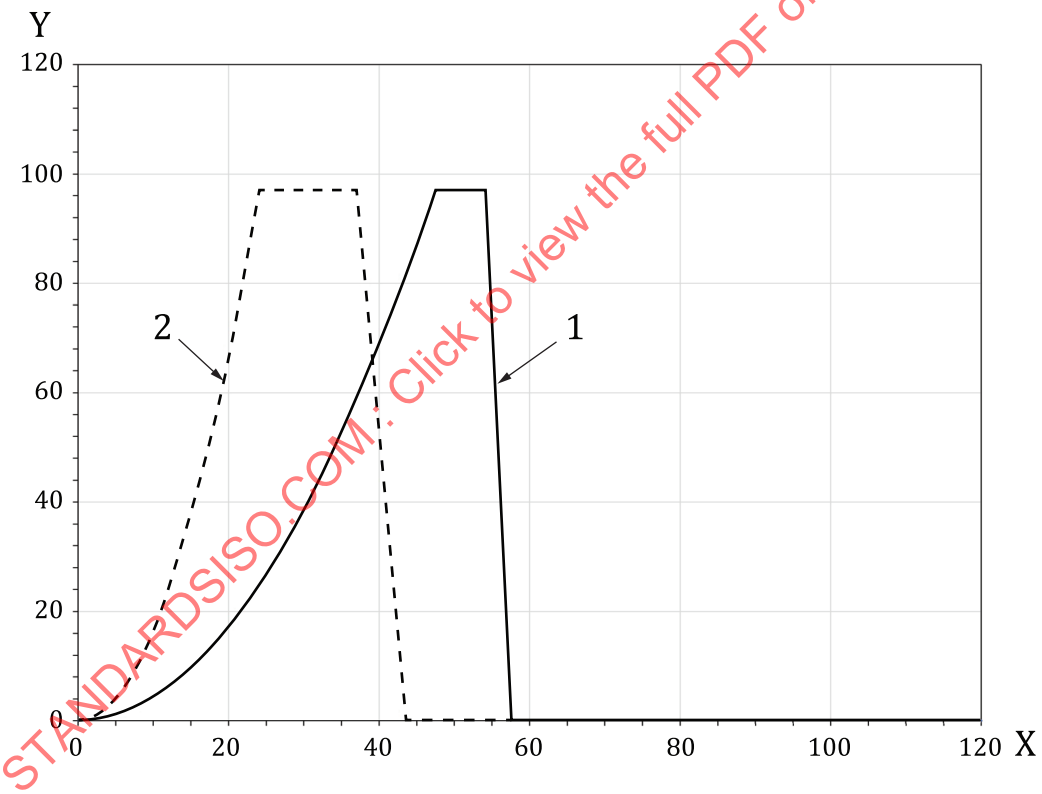

Key

X time (min)
Y heat release rate (MW)
1 medium t^2 (4 windows open)
2 fast t^2 (4 windows open)

Figure 8 — Design fire HRR curves from medium and fast t^2-fires (scenario 1) according to simplified formulae

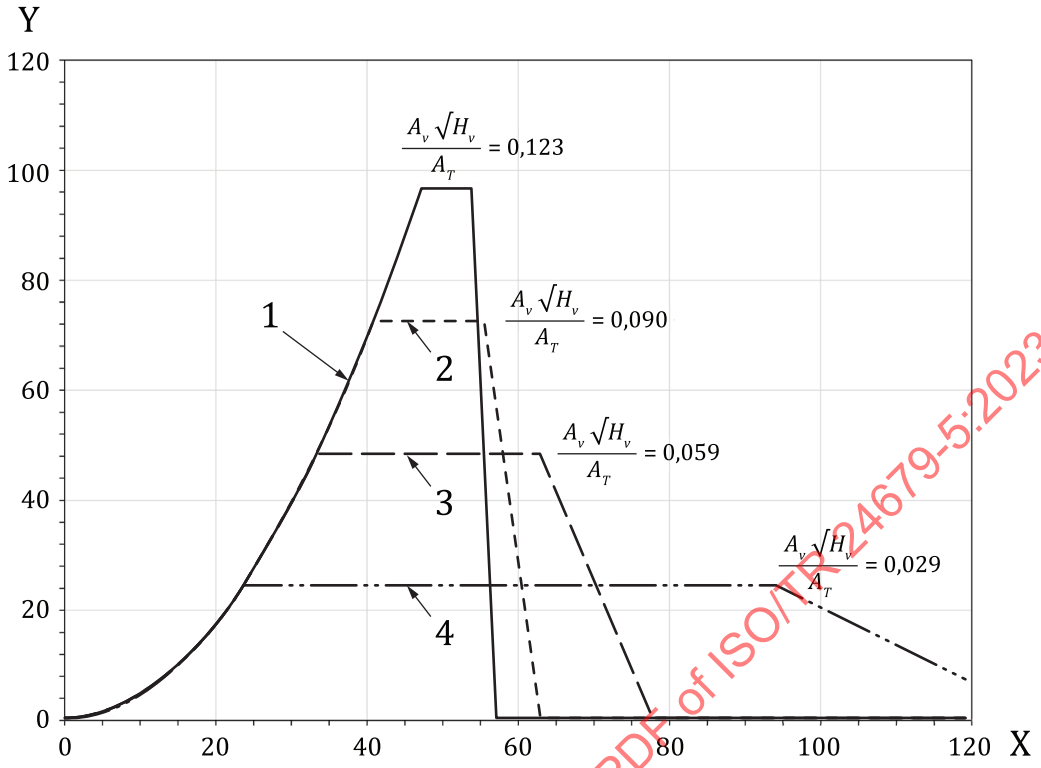

Key

X time (minutes)
Y heat release rate (MW)
1 medium t^2 (4 windows open)
2 medium t^2 (3 windows open)
3 medium t^2 (2 windows open)
4 medium t^2 (1 window open)

Figure 9 — Design fire HRR curves as a function of window openings (scenario 1) according to simplified formulae

5.4.3.1.1 Flashover conditions

An important phenomenon occurring during a fire is the transition to flashover conditions within the compartment of fire origin. According to ISO 24678-6, the heat release rate for flashover conditions is reached when the measured temperature at the hot layer ranges between 500 °C to 600 °C and radiant heat flux to the floor surface exceeds 20 kW/m^2. At these conditions, it is presumed that common combustible materials will ignite after a short time.

While the office floor area of 192 m^2 is beyond the range of experimental datasets used for developing McCaffrey's formulation, the latter is assumed applicable for this example. His empirical correlation assumes that flashover occurs when an upper layer gas temperature reaches 600° (refer to ISO 24678-6:2016, A.3.4). The heat release rate for flashover conditions, $\dot{Q}_{fo}$, calculated using Formula (11), is 20,7 MW.

$$\dot{Q}_{fo} = 740\sqrt{h_T}\sqrt{\frac{A_T}{A\sqrt{H}}}A\sqrt{H} \tag{11}$$

where

A is the total area of openings (48,2 m^2);

H is the average height of all openings (1,8 m);

h_T is the average heat transfer coefficient (kW m^{-2} K^{-1});

A_T is the total area of the enclosure excluding area A_V (527,8 m^2).

Formula (12) is used to estimate the average effective heat transfer coefficient, h_T, of the interior surfaces, taken as 0,022 8 kW m^{-2} K^{-1}.

$$h_T \approx \frac{A_{wc}}{A_T}\sqrt{\frac{(k\rho c)_{wc}}{t_c}} + \frac{A_f}{A_T}\sqrt{\frac{(k\rho c)_f}{t_c}} \quad (12)$$

where

A_{wc} is the area of the walls and ceiling protected by Type X gypsum board (384 m^2);

A_f is the floor area consisting of hardwood flooring (192 m^2);

$(k\rho c)_{wc}$ is the Type X gypsum board thermal inertia used on the walls and ceiling (0,593 kW^2s/m^4K^2);

$(k\rho c)_f$ is the hardwood flooring thermal inertia (0,196 kW^2s/m^4K^2);

t_c is the characteristic time for flashover occurrence (1 000 s).

According to the design fire curves shown in Figure 8, Q_{fo} is reached at 21,9 min (medium t^2-fire) and 11,1 min (fast t^2-fire).

5.4.3.2 Design fire for scenario 2 (CFD modelling)

CFD modelling was performed using Fire Dynamics Simulator (FDS).[24] The design fire assumes a representative distribution of the fuel load based on a uniform distribution of the 28 cubicles across the floor area and the engineered hardwood flooring. All CFD modelling scenarios assumed that fire is initiated by a cubicle located near the centre of the floor area, as shown in Figure 10.

This floor configuration results in having the cubicle of fire origin located directly beneath the mid-span of a timber beam. It represents one specific scenario of which the effects of the resulting fire are being analyzed. A detailed performance-based fire engineering design would require the evaluation of several other floor configurations and their impacts on the structural elements.

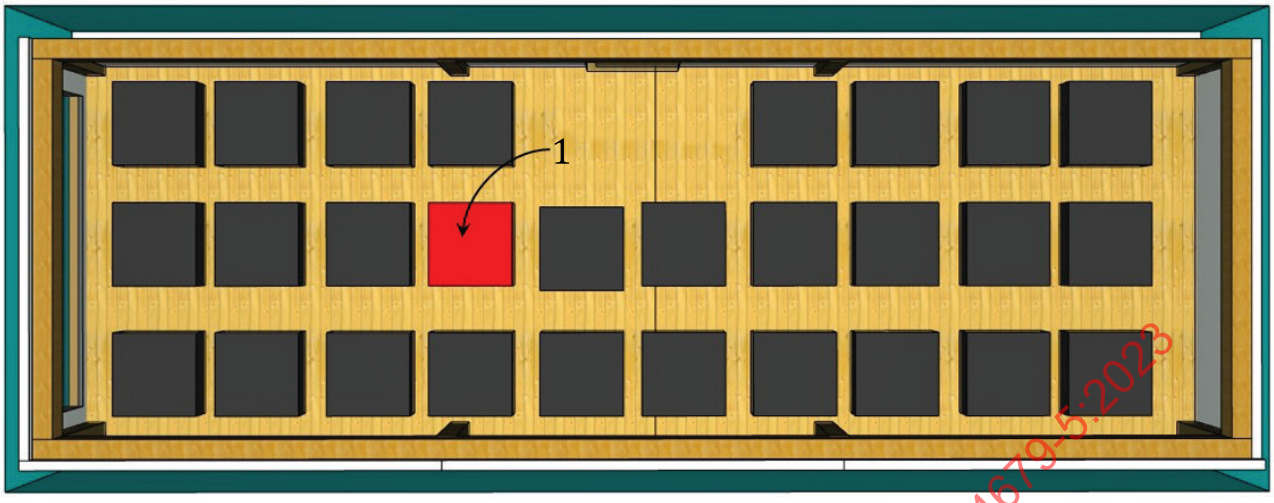

Key

1 cubicle of fire origin

Figure 10 — Floor configuration showing cubicle of fire origin, as displayed in FDS

In scenario 2, the fire is characterized by the actual contribution of all 28 cubicles igniting one after the other, following their own respective HRR as shown in Figure 6 b). Except for the cubicle of fire origin being the first item ignited, each cubicle was set to ignite afterwards when its surface temperature reached 380 °C. A NIST study conducted on single office workstations reported office components ignition temperatures ranging from 290 °C to 407 °C, with an average value of 370 °C.[25] However, the average ignition temperature increases to 385 °C when neglecting the carpet ignition temperature of 290 °C. The flooring in this example is made of engineered hardwood flooring. As such, an ignition temperature of 380 °C is deemed appropriate for the CFD modelling.

The resulting HRR curve from the CFD modelling is shown in Figure 11. It can be observed that the fire development curve is similar to a medium t^2-fire curve when following the scenario 1 methodology. However, the peak of HRR is much higher using a t^2-fire (with 4 windows open) when compared to that provided from CFD modelling. The CFD modelling results in a peak HRR slightly higher than 60 MW.

The CFD modelling of scenario 2 provides a total energy of 110,595 MJ, representing a consumed fuel load density of 576 MJ/m^2. This value is much lower than the design FLED of 735 MJ/m^2, suggesting that the fire is under-ventilated during its development phase and thus does not result in a complete combustion of the pyrolysis gases produced by the available combustibles within the fire compartment (but potentially outside). The CFD modelling is nevertheless more consistent with a medium t^2-fire presuming only 2 or 3 windows opened, as shown in Figure 11.

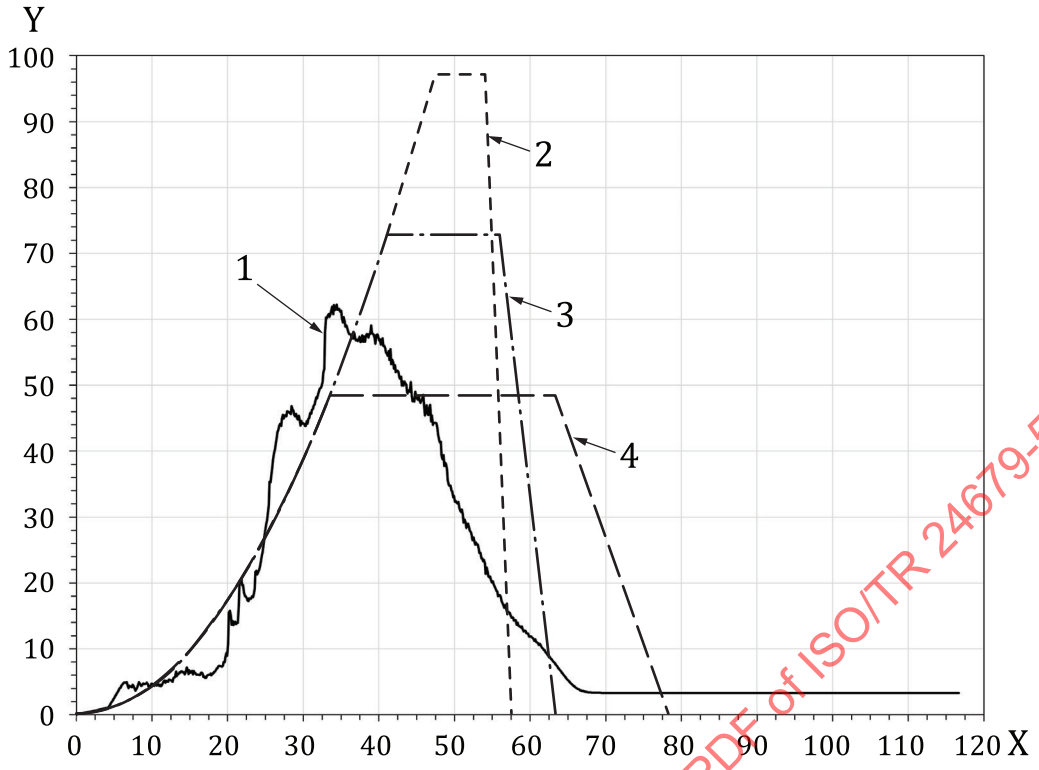

Key

X	time (min)	2	medium t^2 (4 windows open)
Y	heat release rate (MW)	3	medium t^2 (3 windows open)
1	CFD modelling	4	medium t^2 (2 windows open)

Figure 11 — Design HRR fire curve for scenario 2 according to CFD modelling and the comparison to HRR fire curves defined for medium t^2-fires according to simplified formulae

5.4.3.2.1 Flashover conditions

In attempts to evaluate the time at which flashover occurred during the CFD modelling, 6 radiative heat flux devices and 6 hot layer temperature devices were simulated across the floor area (Figure 12 and Figure 13). The radiative heat flux sensors were positioned upward at the floor level and the hot layer temperature devices were set to measure the upper layer temperature. Table 3 provides the times at which 20 kW/m^2 was recorded by the heat flux devices at the floor level and at which the upper layer reached a temperature of 500 °C and 600 °C.

The CFD modelling provides minimum and average times to reach 20 kW/m^2 of 21,5 min and 25,4 min, respectively. At these times, the HRR of the design fire is 23,8 MW and 37,7 MW, respectively.

The minimum and average times for reaching an upper layer temperature of 500 °C were 16,3 min and 20,2 min, corresponding to HRR of 7,3 MW and 17,1 MW, respectively. The minimum and average times for reaching an upper layer temperature of 600 °C were 20,2 min and 21,6 min, corresponding to HRR of 17,1 MW and 23,9 MW, respectively.

Given the large open floor space, the range of times to reach a given temperature threshold can be quite large, as observed through this CFD modelling. As such, it can be argued that determining flashover conditions using the 20 kW/m^2 criterion is likely to be more reasonable. The minimum time of 21,5 min for reaching flashover conditions is a conservative assumption and is consistent with the calculated value of 21,9 min, assuming a medium t^2-fire. The HRR rates at these times to flashover conditions were 23,8 MW and 20,7 MW when determined from the CFD modelling and a medium t^2-fire, respectively. These times and HRR ignore any contribution of the timber structural elements to the fire.

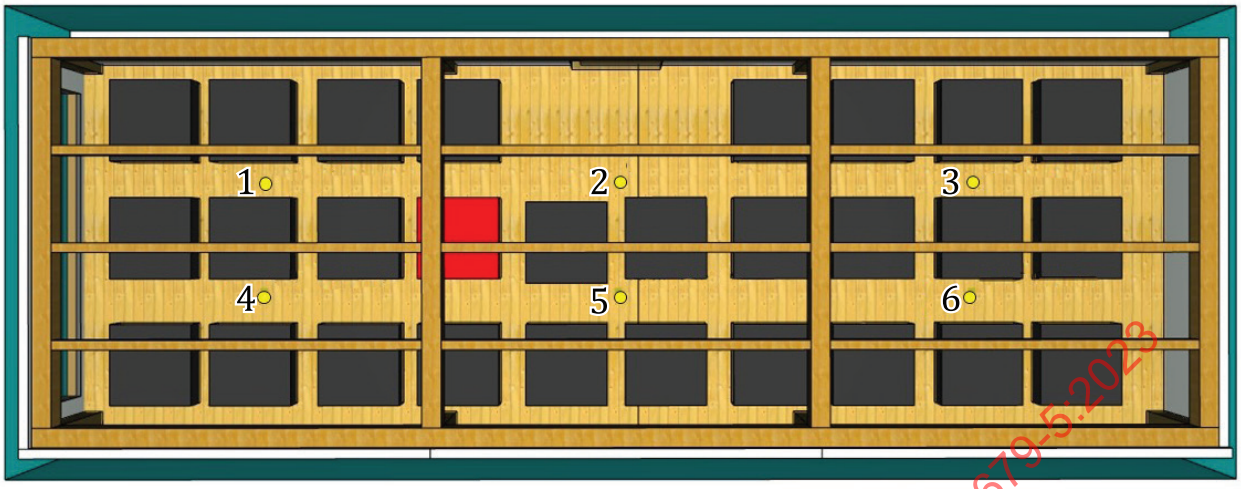

Key

1	floor flux 01	2	floor flux 02	3	floor flux 03
4	floor flux 04	5	floor flux 05	6	floor flux 06

Figure 12 — Heat flux sensor at floor level

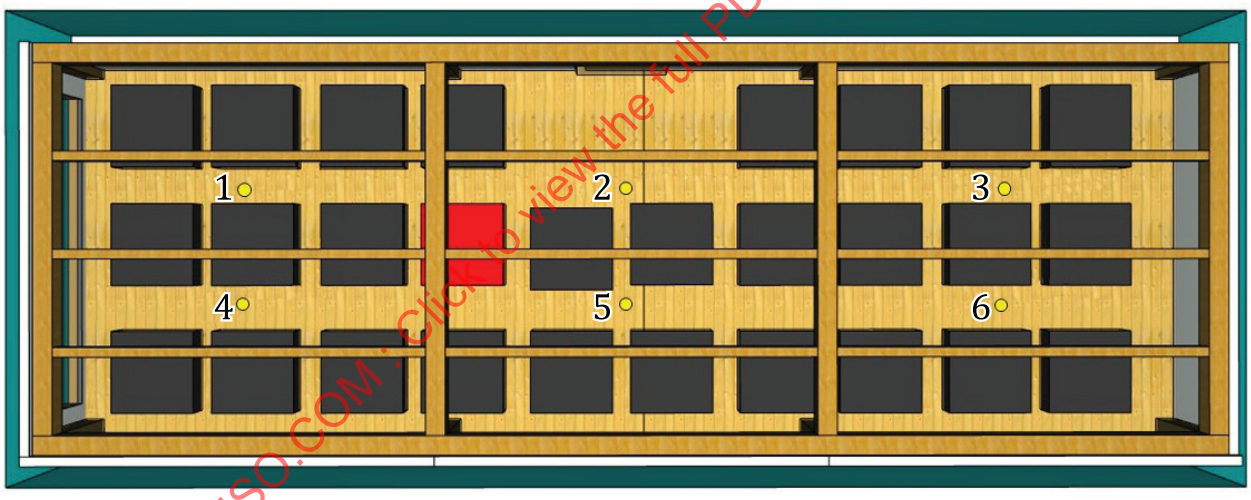

Key

1	layer 01	2	layer 02	3	layer 03
4	layer 04	5	layer 05	6	layer 06

Figure 13 — Layer probe for temperature of upper layer

Table 3 — Flashover conditions from CFD modeling (scenario 2)

Device	Floor radiative heat flux sensor	Upper layer temperature	
	Time to 20 kW/m²	Time to 500 °C	Time to 600 °C
1	24,4 min	20,7 min	22,6 min
2	26,0 min	20,2 min	20,2 min
3	33,7 min	26,0 min	29,1 min
4	21,5 min	19,0 min	21,9 min
5	21,5 min	16,3 min	20,3 min
6	33,7 min	26,0 min	27,3 min
Minimum time	21,5 min	16,3 min	20,2 min
HRR at minimum time	23,8 MW	7,3 MW	17,1 MW
Average time [a]	25,4 min	20,2 min	21,6 min
HRR at average time	37,7 MW	17,1 MW	23,9 MW

[a] Average times are taken from the average radiative heat flux from all 6 sensors and average temperature profile shown in Figure 14.

5.4.3.2.2 Temperature profile

Figure 14 shows the upper layer temperature recorded by the 6 hot layer temperature devices from the CFD modelling. Given that the fire originated at a location closer to the temperature devices 1 to 4, it is expected that the temperatures measured at these locations were to be higher and would reach their peak values faster than devices 3 and 6.

Moreover, it can be observed that maximum temperatures in the range of (1 000 - 1 300) °C are obtained, with an average maximum temperature of 1 200 °C. The temperatures generated from the CFD modelling appear to be reasonable for large open plan room fires, while being more severe when compared to test data. Large-scale fire testing of compartments with exposed timber surfaces and floor areas of 83 m²[26] and 42 m²[27] observed ceiling temperatures in the range of (900 - 1 000) °C and (1 000 - 1 100) °C, respectively. It is therefore assumed that the temperatures resulting from the CFD modelling are reasonable.

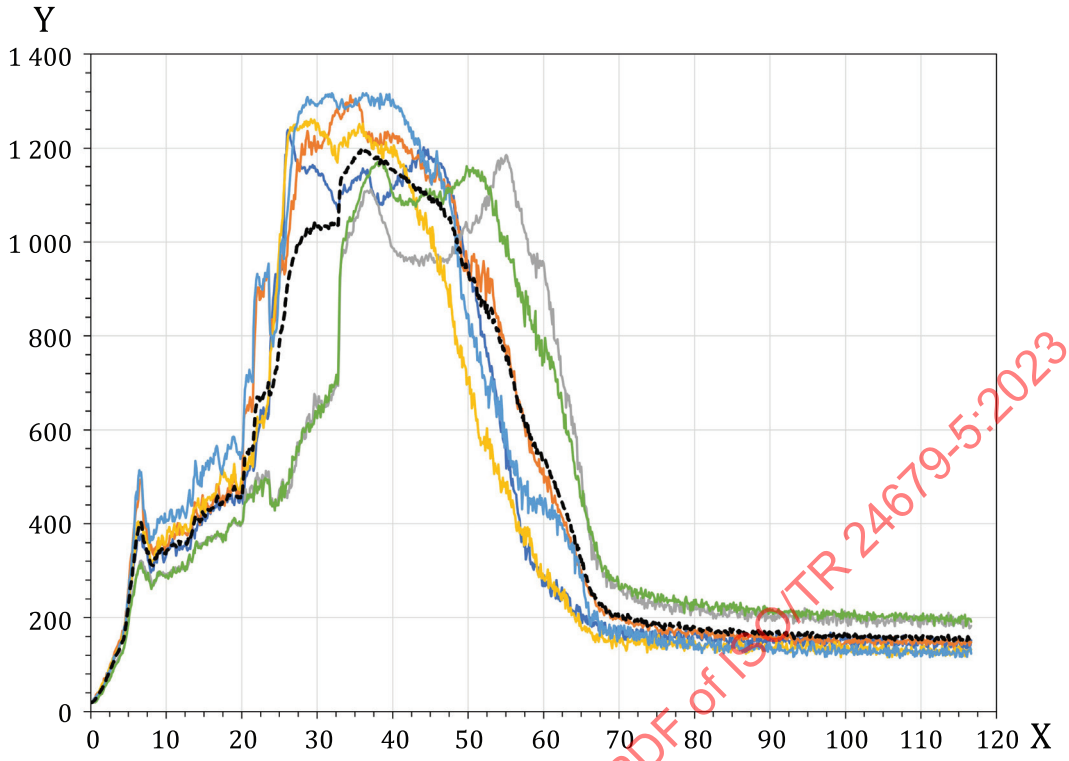

Key

X time (min)
Y upper layer temperature (°C)
upper layer 1
upper layer 2
upper layer 3
upper layer 4
upper layer 5
upper layer 6
upper layer (average)

Figure 14 — Upper layer temperature (scenario 2) according to CFD modelling

5.4.3.2.3 Window glass breakage

During the CFD modelling, all windows were initially closed and their glass was set to open/break when a temperature sensor located at the top of the window reached 500 °C or when the fire became limited by ventilation,[28] whichever occured first. This would automatically change the ventilation factor as a function of time during the CFD modelling. In the CFD modelling, the windows were 0,2 m shorter at the bottom in an attempt to supply enough air to the fire and facilitate its growth. Table 4 provides the times at which each window reached 500 °C, as well as the HRR at that time. It can be observed that windows 1 and 2 broke at approximately the same time when flashover conditions were reached. Window 4 broke shortly after flashover conditions, while Window 3 broke while the fire development was in its steady-state phase.

Table 4 — Breakage time of window glass from CFD modelling (scenario 2)

Window	Time to 500 °C	HRR at time to 500 °C
1	22,9 min	24,8 MW
2	21,4 min	20,7 MW
3	33,6 min	58,5 MW
4	24,9 min	33,2 MW

5.4.3.2.4 Fall-off of gypsum board

In the event that combustible structural elements become exposed to fire, they can ignite and contribute to fire growth and severity. In this example, a limited portion of the primary beams and columns are initially exposed for aesthetic purposes. The secondary elements are protected by a single layer of 16 mm Type X gypsum boards (i.e. fire-resistance rated gypsum boards).

When performing the CFD modelling, the gypsum boards are assumed to be falling-off when their back-surface temperature reaches 600 °C.[29] At that time, the non-combustible insulation inside the cavities would also be falling-off, suddenly exposing secondary structural elements and decking to fire. Figure 15 illustrates the position of the 16 temperature devices used to record the temperature at the interface between the back-surface of the Type X gypsum boards and insulating material in the cavities. Figure 16 illustrates the temperature profiles recorded at the back-surface of the gypsum boards. Table 5 provides the times to reach 300 °C and 600 °C as well as the maximum temperatures reached at each back-surface of the gypsum boards. From the CFD modelling, no gypsum board would have failed during the entire fire duration. However, all temperatures were beyond the wood charring temperature of 300 °C, suggesting that secondary timber beams (B2) had potentially started to char shortly after flashover conditions were reached. However, charring that can have started on the secondary beams would be considerably reduced due to the thermal protection afforded by the gypsum boards that remained in place. The predictions are consistent with actual large-scale mass timber compartments fire tests where failure (fall-off) of gypsum boards was also not observed.[26],[30] The transient heat transfer through the Type X gypsum boards was performed using the implied heat transfer process of the CFD modeling and assumed constant thermal properties. Using constant thermal properties typically results in conservative predictions as they do not explicitly consider moisture migration and calcination of the gypsum core.

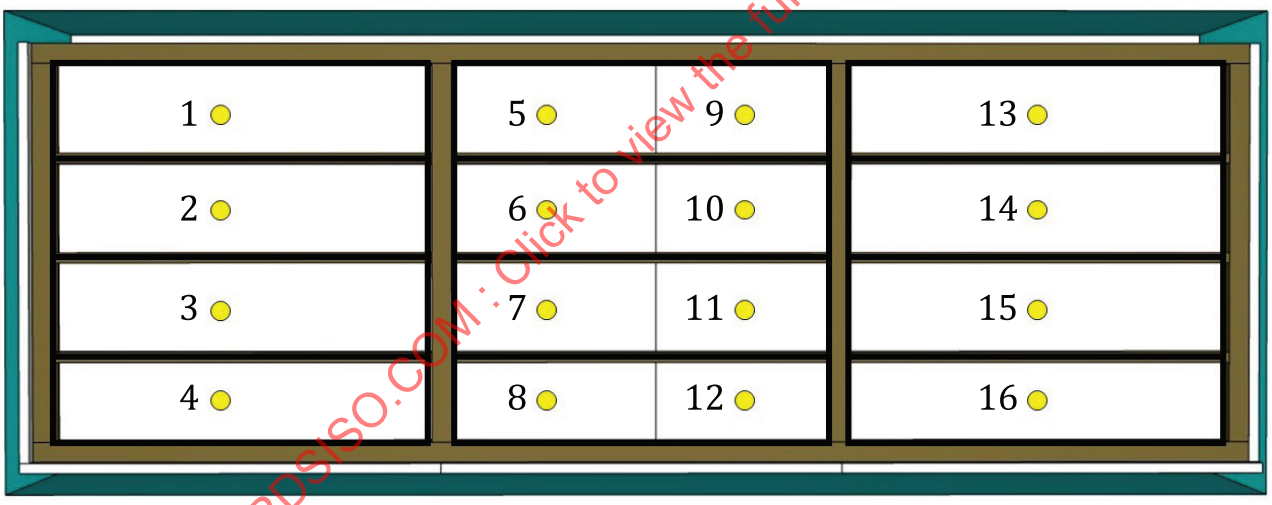

Key

1-16 temperature devices

Figure 15 — Gypsum board (ceiling) configuration

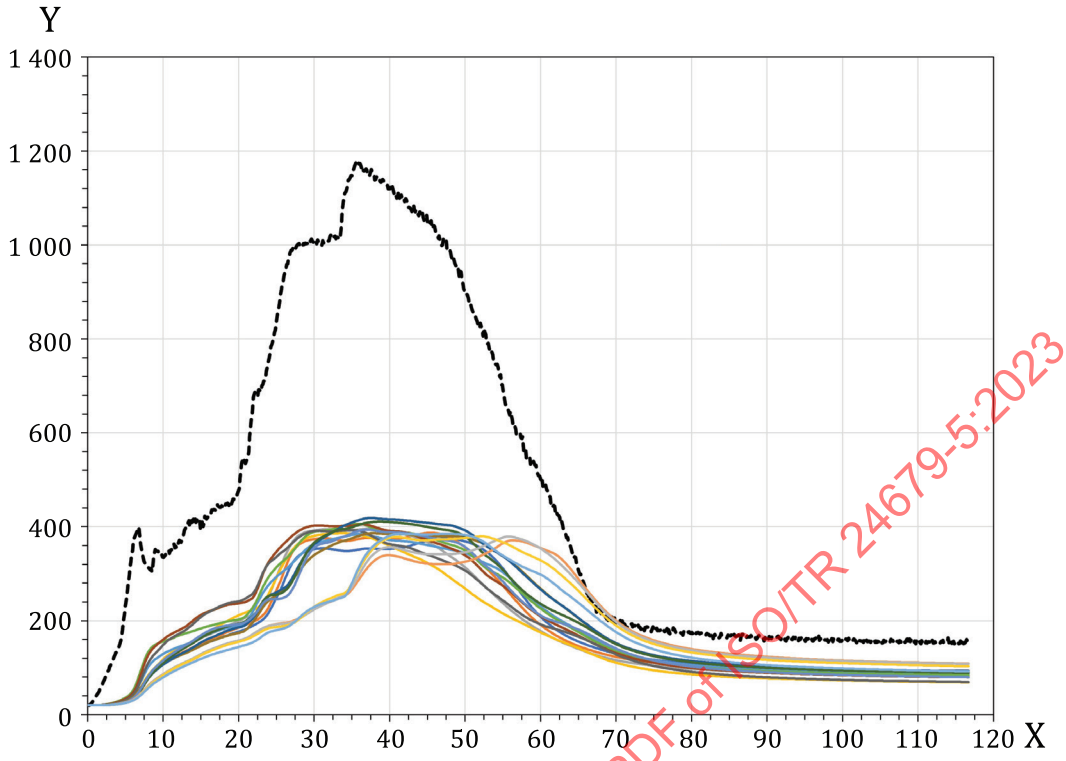

Key

X time (min)
Y temperature (°C)
upper layer (average)
back surf 01
back surf 02
back surf 03
back surf 04
back surf 05
back surf 06
back surf 07
back surf 08
back surf 09
back surf 10
back surf 11
back surf 12
back surf 13
back surf 14
back surf 15
back surf 16

Figure 16 — Temperature at back-surface of Type X gypsum boards (scenario 2)

Table 5 — Thermal performance of gypsum boards from CFD modelling (scenario 2)

Gypsum board	Time to 300 °C	Maximum temperature at back-surface of Type X gypsum boards
1	26,5 min	375 °C
2	25,9 min	387 °C
3	25,2 min	395 °C
4	25,3 min	386 °C
5	25,6 min	385 °C
6	24,4 min	406 °C
7	23,3 min	405 °C
8	23,2 min	393 °C

Table 5 *(continued)*

Gypsum board	Time to 300 °C	Maximum temperature at back-surface of Type X gypsum boards
9	27,8 min	386 °C
10	27,4 min	419 °C
11	27,0 min	411 °C
12	28,1 min	394 °C
13	36,5 min	371 °C
14	36,1 min	379 °C
15	35,7 min	380 °C
16	35,6 min	385 °C

5.4.3.3 Design fire for scenario 3 (CFD modelling)

Scenario 3 is essentially the same as scenario 2, characterized by the actual contribution of all 28 cubicles igniting one after the other, following their own respective HRR as shown in Figure 6b). In addition, the contribution from the structural timber elements is considered and thereby increasing the actual fire load density. During the CFD modelling, the reaction properties of the timber elements assume a HRR contribution based on cone calorimeter test data[31] and an ignition temperature of 343 °C, as calculated per[32].

The resulting HRR curve from the CFD modelling is shown in Figure 17. It can be observed that the fire development curve remains like a medium t^2-fire curve when following scenario 1 methodology, until the HRR reaches approximately 16 MW, which is before flashover conditions are reached. After that time, the HRR increases at a faster rate, approximately half-way between a medium and fast t^2-fire. The peak HRR is estimated at approximately 65 MW, which is about 5 MW higher than scenario 2, as shown in Figure 18. Globally, the full fire development is similar for both scenarios, with a slight difference in growth rate and peak HRR, which can be attributed to the timber contribution explicitly considered in scenario 3.

The CFD modelling of scenario 3 provided a total energy of 116,486 MJ, representing a consumed fuel load density of 607 MJ/m^2. This represents an 5 % increase when compared to scenario 2. Nevertheless, this value remains lower than the design FLED of 735 MJ/m^2, suggesting that the fire is under-ventilated during its development phase and thus does not result in a complete combustion of the available combustibles. The difference between both scenarios is also deemed reasonable given the low amount of exposed structural timber elements in the office suite (±3 % of the total area of the compartment, excluding openings).

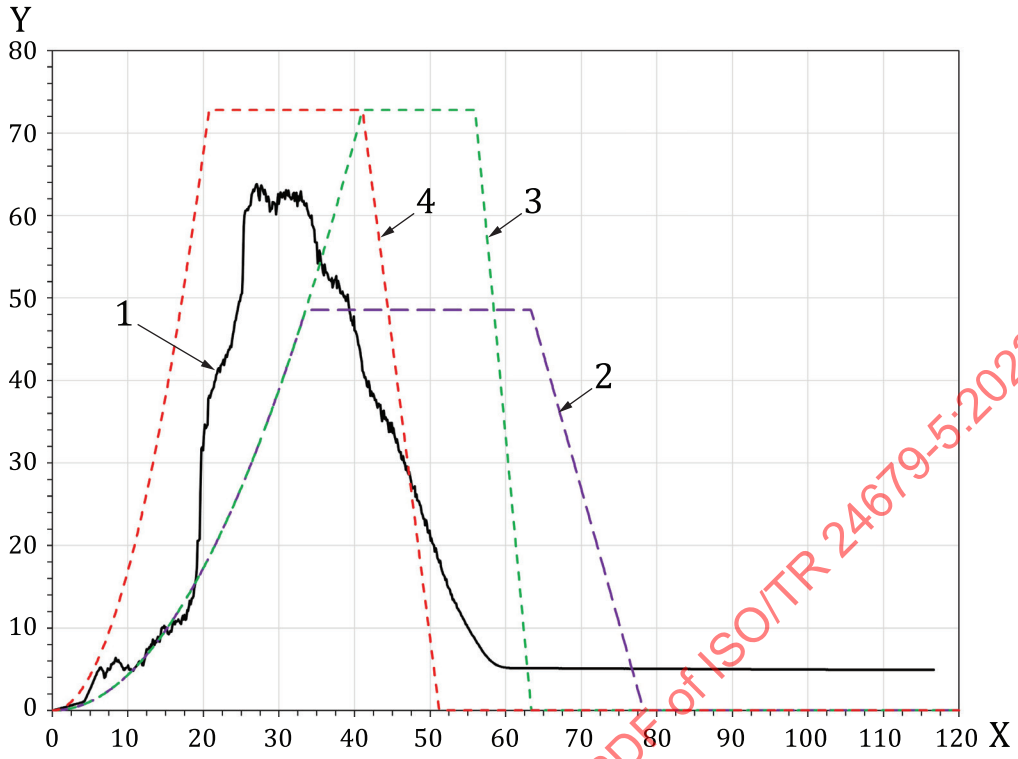

Key

X	time (min)	2	medium t^2 (2 windows open)
Y	heat release rate (MW)	3	medium t^2 (3 windows open)
1	CFD modelling (scenario 3)	4	fast t^2 (3 windows open)

Figure 17 — Design HRR fire curve for scenario 3 according to CFD modelling and the comparison to HRR fire curves defined for medium and fast t^2-fires according to simplified formulae

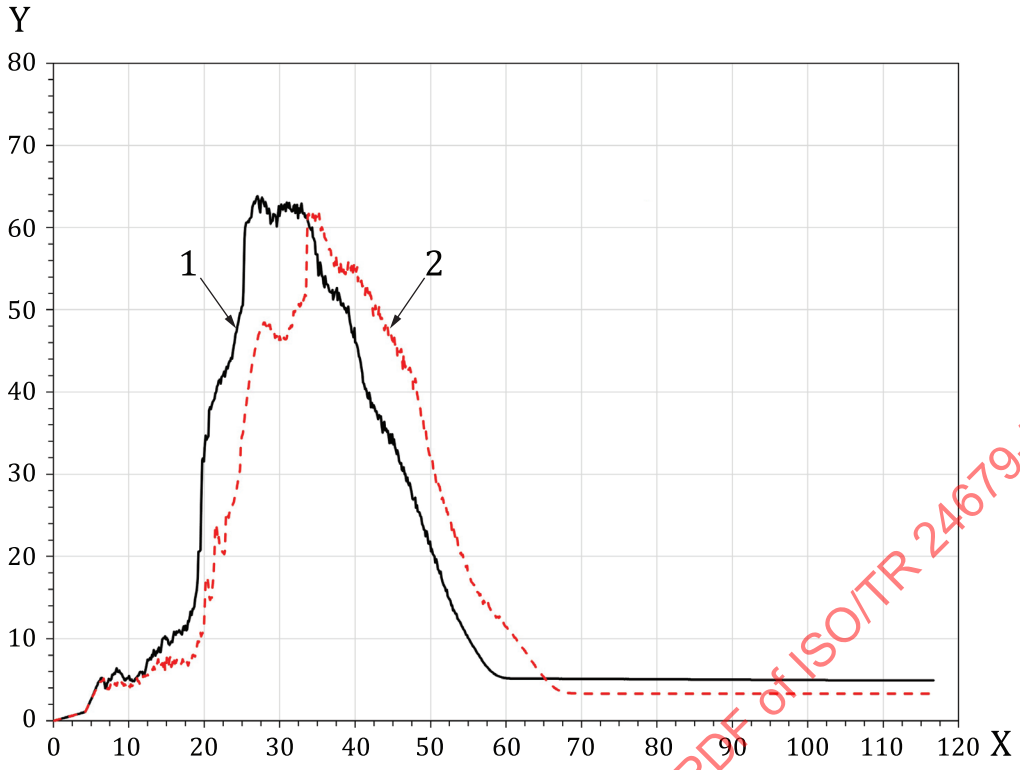

Key

X time (min)
Y heat release rate (MW)
1 CFD modelling (scenario 3)
2 CFD modelling (scenario 2)

Figure 18 — Heat release rates: scenario 2 compared to scenario 3

5.4.3.3.1 Flashover conditions

The same 6 radiative heat flux devices and hot layer temperature devices from scenario 2, as well as their location within the compartment, are used to assess flashover conditions from the CFD modelling of scenario 3. Table 6 provides the times at which 20 kW/m^2 was recorded by the heat flux devices at the floor level and at which the upper layer reached a temperature of 500 °C and 600 °C.

The CFD modelling provides minimum and average times to reach 20 kW/m^2 of 19,4 min and 19,6 min, respectively. At these times, the HRR of the design fire is 20,6 MW and 26,3 MW, respectively. Flashover conditions are reached faster than in scenario 2, where the minimum time was 21,5 min and the average time was 25,4 min. At the minimum times to reach flashover conditions from both scenarios 2 and 3, the HRR were 23,8 MW and 20,6 MW, respectively, which is consistent with the calculated value of 20,7 MW reached at 21,9 min, when assuming a medium t^2-fire. When comparing the HRR at the average times to flashover conditions from both scenarios 2 and 3 (37,7 MW and 26,3 MW, respectively), it can be observed that it takes 5,8 min longer to reach that HRR in scenario 2. The HRR for both scenarios, as shown in Figure 18, suggests that timber elements considered in scenario 3 started contributing to fire growth and intensity shortly after 12 min, the time at which both curves start deviating from each other. Figure 19 shows the graphical representation of the fire obtained from the CFD modelling.

The minimum and average times for reaching an upper layer temperature of 500 °C were 14,6 min and 17,3 min, corresponding to HRR of 10,1 MW and 11,5 MW, respectively. The minimum and average times for reaching an upper layer temperature of 600 °C were 19,0 min and 19,7 min, corresponding to HRR of 15,9 MW and 31,7 MW, respectively.

As observed from the CFD modelling of scenario 2, the range of times to reach a given temperature threshold can be quite large. It can also be observed that determining flashover conditions using the 20 kW/m^2 criterion is likely to be more reasonable approach rather than using a temperature threshold. The minimum time of 19,4 min for reaching flashover conditions is a conservative assumption and is consistent to the calculated value of 21,9 min, assuming a medium t^2-fire. The HRR at 19,4 min from CFD modelling and at the calculated time of 21,9 min are 20,6 MW and 20,7 MW. These values are considered to be reasonable, given that Scenario 3 considered a greater fuel load (607 MJ/m^2) when compared to that of Scenario 2 (576 MJ/m^2). A shorter time to flashover conditions is thus to be expected.

Table 6 — Flashover conditions from CFD modelling (scenario 3)

Device	Floor radiative heat flux sensor	Upper layer temperature	
	Time to 20 kW/m^2	Time to 500 °C	Time to 600 °C
1	20,8 min	17,3 min	19,4 min
2	24,3 min	16,2 min	19,8 min
3	25,3 min	20,9 min	22,9 min
4	19,4 min	16,3 min	19,3 min
5	19,6 min	14,6 min	19,0 min
6	25,1 min	21,8 min	23,7 min
Minimum time	19,4 min	14,6 min	19,0 min
HRR at minimum time	20,6 MW	10,1 MW	15,9 MW
Average time [a]	19,6 min	17,3 min	19,7 min
HRR at average time	26,3 MW	11,5 MW	31,7 MW

[a] Average times are taken from the average radiative heat flux from all 6 sensors and average temperature profile shown in Figure 20.

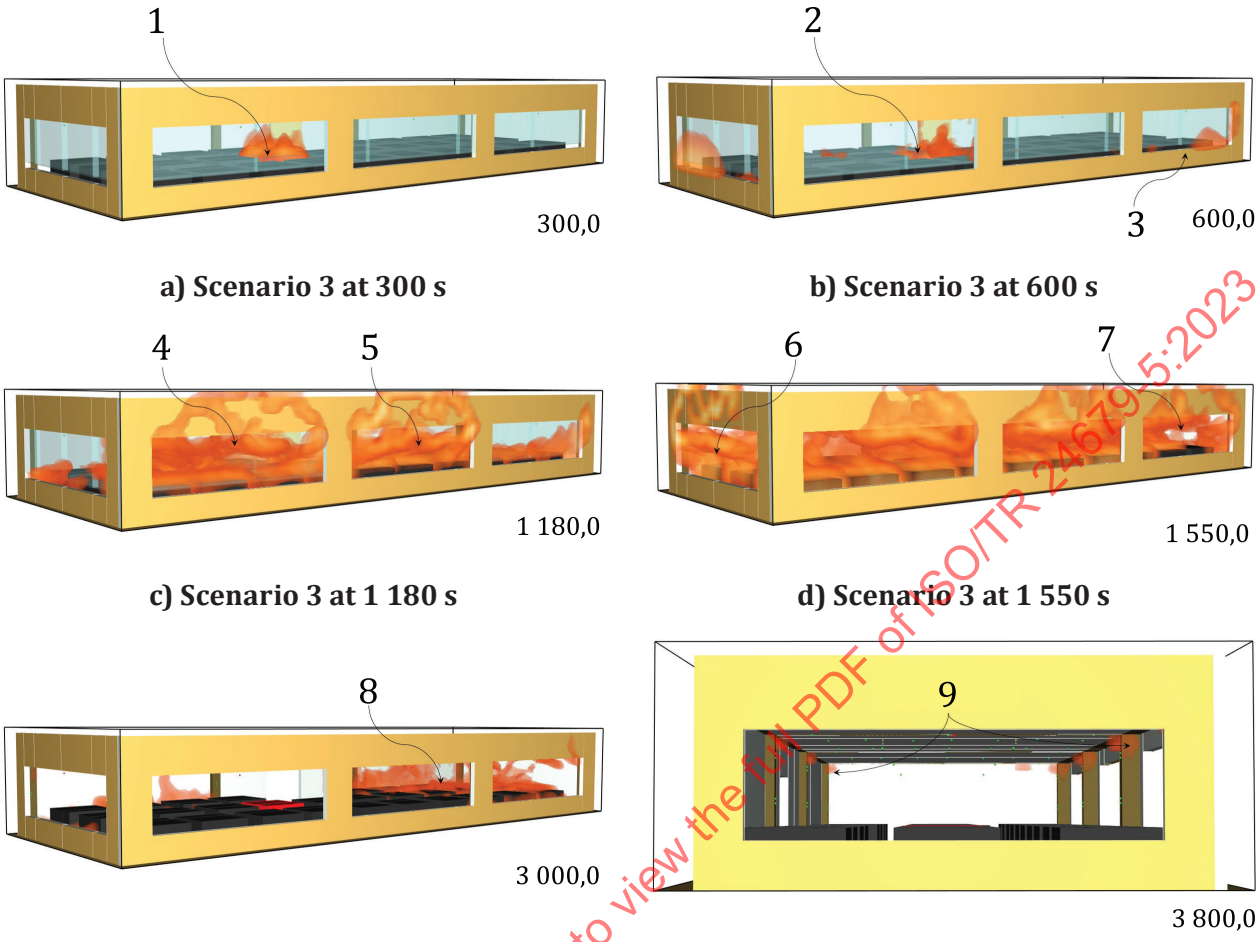

a) Scenario 3 at 300 s

b) Scenario 3 at 600 s

c) Scenario 3 at 1 180 s

d) Scenario 3 at 1 550 s

e) Scenario 3 at 3 000 s

f) Scenario 3 at 3 800 s

Key

1 cubicle of fire origin
2 cubicle of fire origin
3 air leakage on purpose to facilitate fire growth (air entrainment)
4 opening of window 1 at 19,6 min (1 176 s)
5 opening of window 2 at 19,1 min (1 146 s)
6 opening of window 4 at 20,7 min (1 242 s)
7 opening of window 3 at 25,2 min (1 512 s)
8 fire decaying towards to back of the office space
9 persisting flaming on timber elements

Figure 19 — Graphical representation from CFD modelling (scenario 3)

5.4.3.3.2 Temperature profile

The same 6 hot layer temperature devices from scenario 2, as well as their location within the compartment, are used to assess the temperature of the upper layer temperature from the CFD modelling of Scenario 3 (Figure 20).

As with scenario 2, it can be observed that the maximum temperatures obtained from the CFD modelling are in the range of (1 000 - 1 300) °C, with an average maximum temperature of 1 200 °C. The

temperatures appear to be more severe when compared to test data, as previously discussed in 5.4.3.2.2. It is therefore assumed that the temperatures resulting from the CFD modelling are reasonable.

Figure 21 shows the average upper layer temperatures for scenarios 2 and 3. It can also be observed that the upper layer temperatures are similar until flashover is reached. After that point, the temperature for scenario 3 exhibits a faster increase, most likely due to the timber contribution to fire growth. Nevertheless, the peak temperatures are in the same magnitude for both scenarios. The decay period for scenario 3 appears to be initiated earlier than that of scenario 2 and be following a similar decay rate.

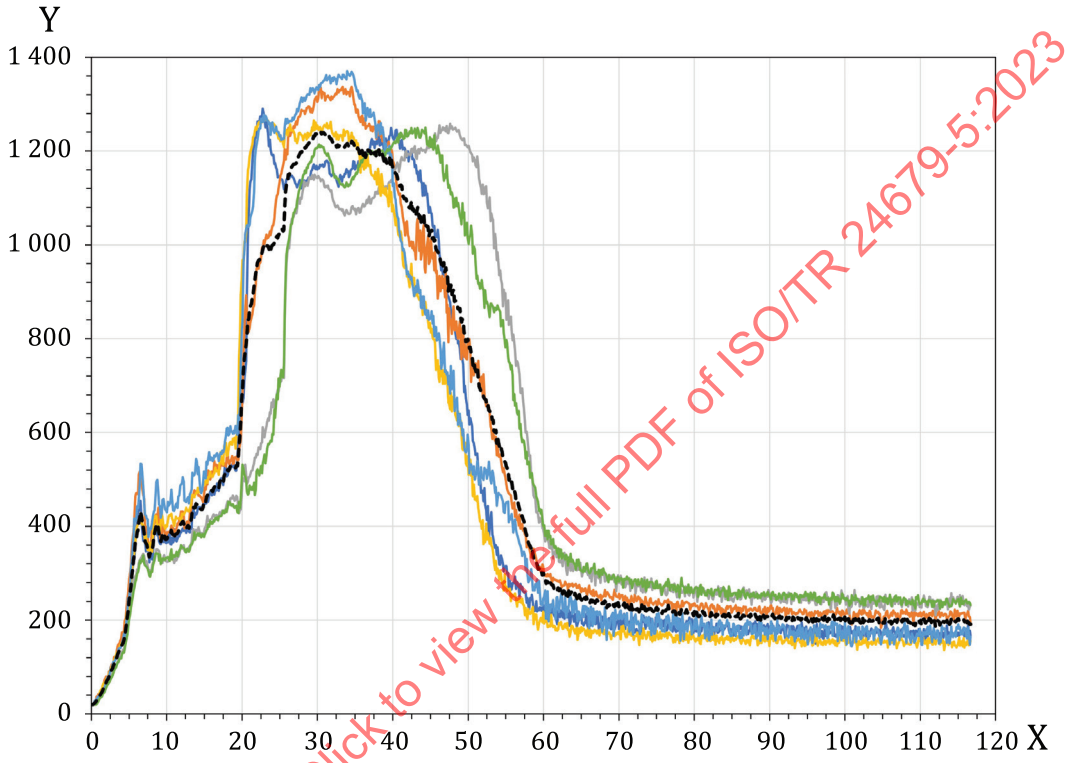

Key

X time (min)
Y upper layer temperature (°C)
upper layer 1
upper layer 2
upper layer 3
upper layer 4
upper layer 5
upper layer 6
upper layer (average)

Figure 20 — Upper layer temperature (scenario 3) according to CFD modelling

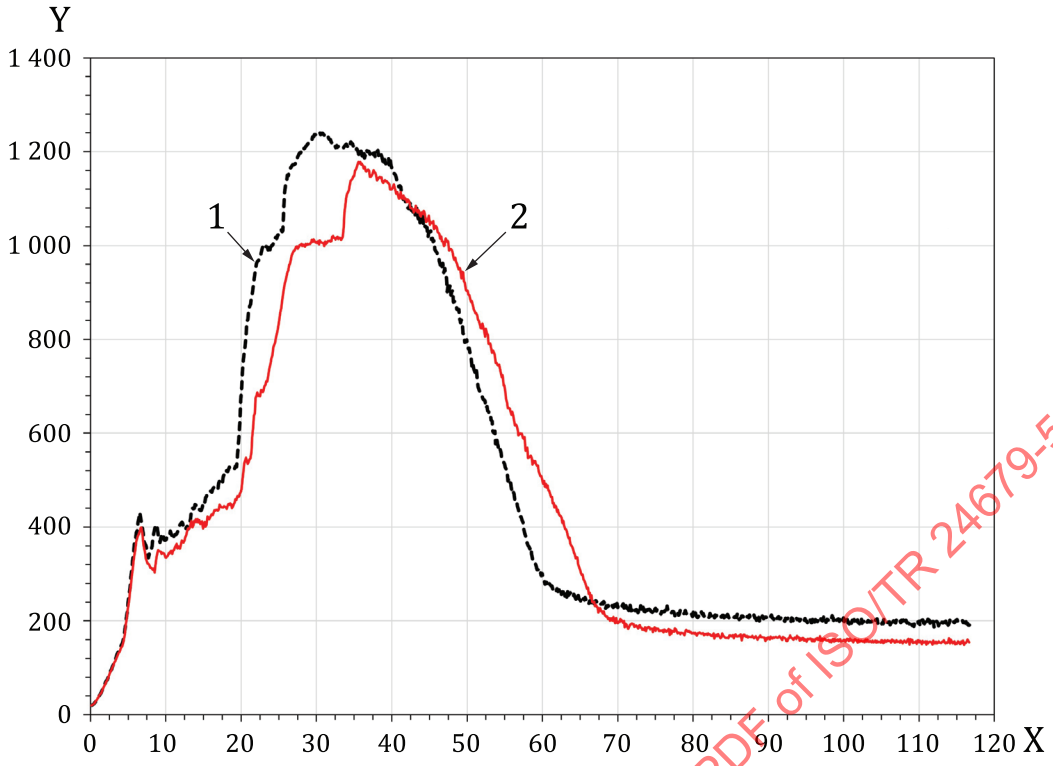

Key

X time (min)
Y upper layer temperature (°C)
1 CFD modelling (scenario 3)
2 CFD modelling (scenario 2)

Figure 21 — Upper layer temperatures: scenario 2 compared to scenario 3

5.4.3.3.3 Window glass breakage

Following the same temperature criterion as scenario 2, the times at which the windows are presumed to break are presented in Table 7. It can be seen that windows 1, 2 and 4 break at approximately 20 min, which coincides with the time at which the HRR development curve (Figure 17) showed a faster increase when flashover conditions were reached. Window 3 breaks after flashover conditions were reached and while the fire development was in its steady-state phase.

Table 7 — Breakage time of window glass from CFD modelling (scenario 3)

Window	Time to 500 °C	HRR at time to 500 °C
1	19,6 min	26,3 MW
2	19,1 min	17,3 MW
3	25,2 min	52,4 MW
4	20,7 min	37,8 MW

5.4.3.3.4 Fall-off of gypsum board

Figure 22 illustrates the temperature profiles recorded at the back-surface of the gypsum boards. Table 8 provides the times to reach 300 °C and 600 °C as well as the maximum temperatures reached at each back-surface of the gypsum boards. From the CFD modelling, no gypsum board would have failed during the entire fire duration. However, all temperatures were beyond wood charring temperature

of 300 °C, suggesting that secondary timber beams (B2) can have started to char shortly after flashover conditions were reached. The predictions are consistent with actual large-scale mass timber compartments fire tests where failure (fall-off) of gypsum boards was also not observed.[26],[30] While the temperature profiles suggest that no failure of the gypsum boards is occurring, it is essential to validate whether the screws used to fasten the gypsum boards remain sufficiently penetrated into the underlying timber throughout the time domain.

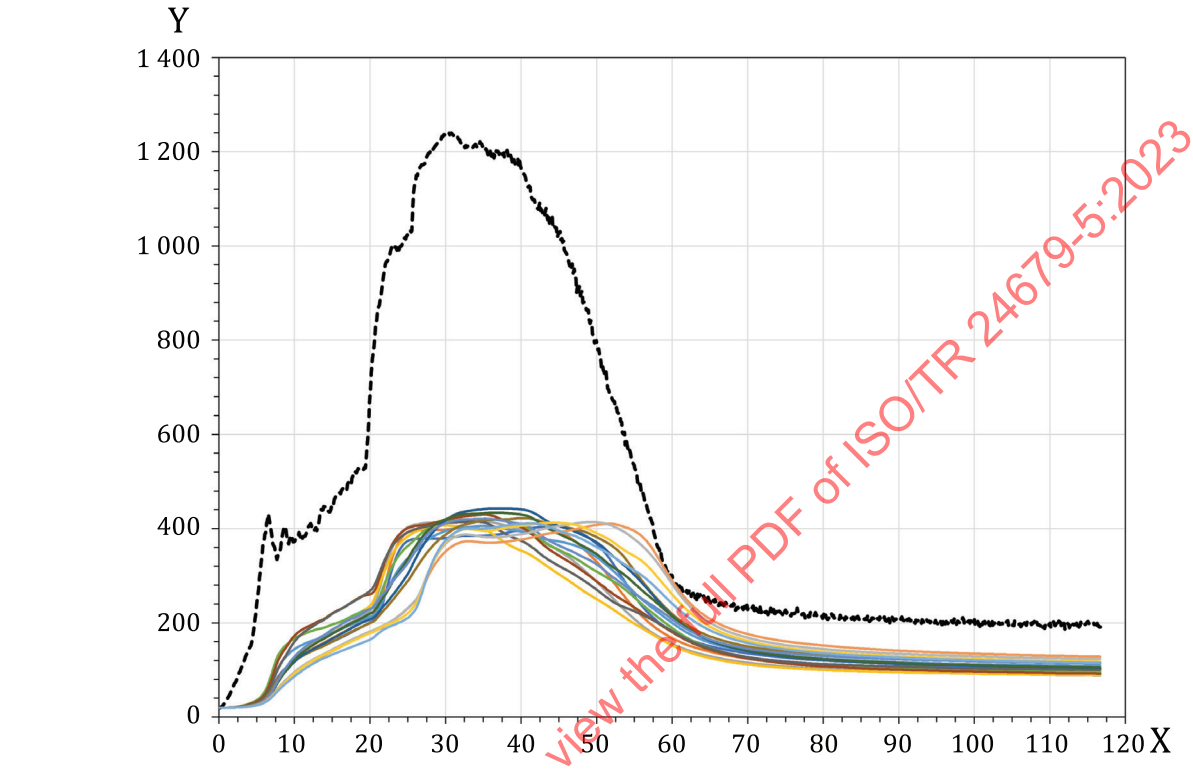

Key

X	time (min)	back surf 08	
Y	temperature (°C)	back surf 09	
	upper layer (average)	back surf 10	
	back surf 01	back surf 11	
	back surf 02	back surf 12	
	back surf 03	back surf 13	
	back surf 04	back surf 14	
	back surf 05	back surf 15	
	back surf 06	back surf 16	
	back surf 07		

Figure 22 — Temperature at back-surface of Type X gypsum boards (scenario 3)

Table 8 — Thermal performance of gypsum boards from CFD modelling (scenario 3)

Gypsum board	Time to 300 °C	Maximum temperature at the back-surface of Type X gypsum boards
1	22,9 min	395 °C
2	22,4 min	399 °C
3	21,8 min	402 °C
4	21,7 min	394 °C
5	23,5 min	394 °C
6	22,5 min	419 °C
7	21,5 min	416 °C
8	21,1 min	402 °C
9	25,7 min	407 °C
10	24,9 min	428 °C
11	23,3 min	419 °C
12	23,6 min	406 °C
13	28,1 min	395 °C
14	27,8 min	399 °C
15	27,7 min	399 °C
16	27,5 min	397 °C

5.4.3.4 Design fire for scenario 4 (CFD modelling)

When automatic sprinklers are installed and activated, they will likely have an impact on the heat release rate of the developing fire by either controlling fire growth or, less likely, extinguishing the fire.

According to ISO/TS 16733-2, when sprinklers activate at a heat release rate greater than 5 MW, they are assumed to have no effect on the fire unless experimental data otherwise supports an impact of the sprinkler on the fire. When sprinklers activate for a fire size of below 5 MW, it can be assumed that the HRR of the design fire remains constant at the value of HRR at time of sprinkler activation for a period of 1 min, reduces to one-third of the HRR at the time of sprinkler activation for another period of 1 minute and remains constant at this latter level thereafter.

In the CFD modelling, two automatic sprinklers were positioned near the cubicle of fire origin, at 5 cm below the gypsum board ceiling level (Figure 23). Each sprinkler was set to activate at a temperature of 68 °C, with a response time index of 80 $(m \cdot s)^{-0,5}$. During scenarios 2 and 3, the automatic sprinklers rapidly activated at an average time of 2,1 min and 2,2 min, respectively. At that time, the heat release rate and temperature of the fire are 0,5 MW and 71 °C for both scenarios. It is noted that only the time of activation was monitored in the CFD modelling. The effect of water suppression was not considered.

Such fire conditions are insufficient for flashover to be reached and for windows to break due to excessive temperature and pressure from hot gases. These conditions are also insufficient to challenge the gypsum boards ceiling and the structural timber elements. Figure 24 shows the heat release rate of scenario 3 without sprinklers and the resulting HRR from sprinklers' activation as per ISO/TS 16733-2. Scenario 3 with sprinklers' activation provided a total energy of 1,184 MJ, representing a consumed fuel load density of 6 MJ/m^2. This represents less than 1 % of the presumed FLED of 735 MJ/m^2.

Given the efficiency of the automatic sprinklers at considerably reducing the fire HRR, flashover conditions, windows breakage, upper layer temperature and fall-off of gypsum boards are not further discussed herein, as they do not occur.

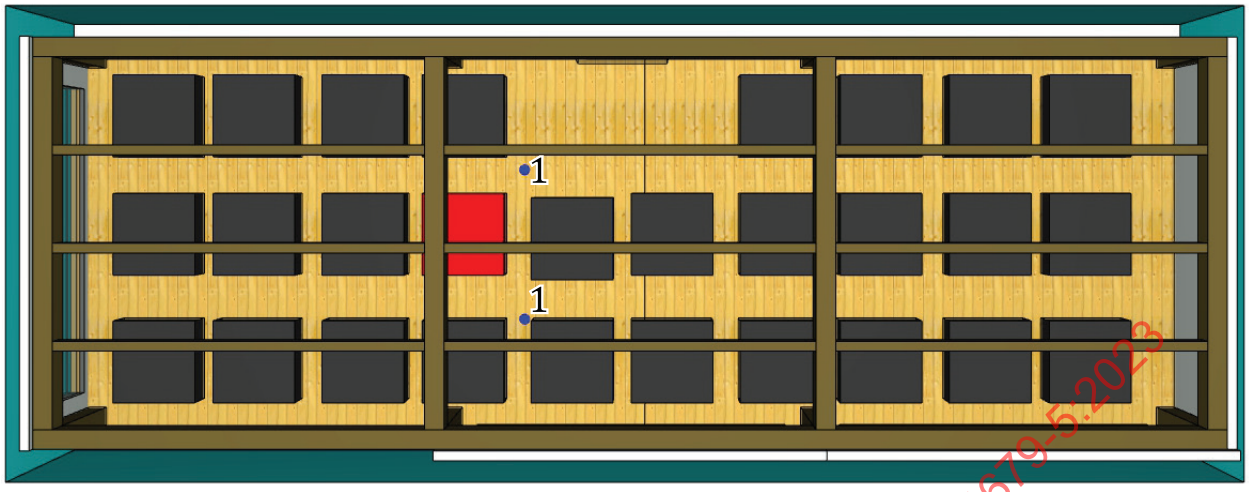

Key

1 SPRK-05

Figure 23 — Location of the automatic sprinklers in CFD modelling

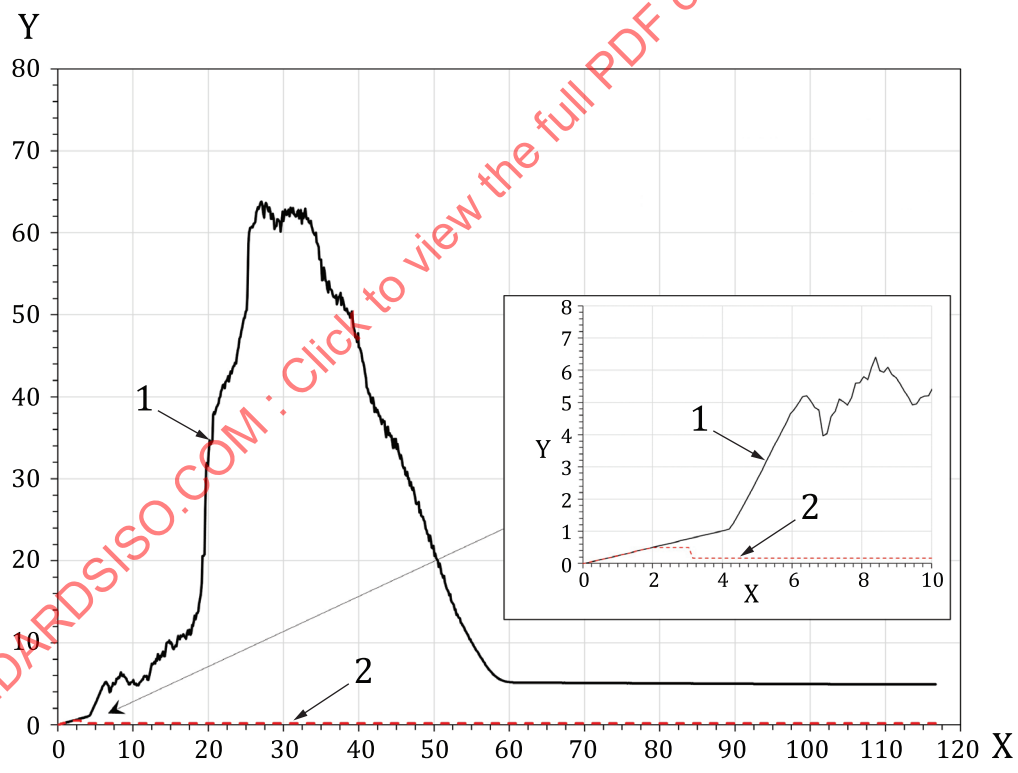

Key

X time (min)

Y heat release rate (MW)

1 scenario 3 (no sprinklers)

2 scenario 4 (with sprinklers)

Figure 24 — Heat release rate of scenario 3, with and without activation of sprinklers

5.5 Step 5: Thermal response of the structure

5.5.1 Charring of timber

When exposed to a sufficient heat source (e.g. fire), timber will experience pyrolysis and ultimately charring. Charring is a fundamental property for timber and is the main parameter used to estimate the load-bearing capacity of structural timber in fire (i.e. residual cross-section method). Piloted ignition of timber occurs at temperatures ranging from (350 - 365) °C for softwoods and (300 - 310) °C for hardwoods.[33] It can also occur when the timber is exposed to a constant heat flux between (10 - 13) kW/m^2,[34,35] with a commonly-accepted critical heat flux for piloted ignition of 12,5 kW/m^2. As mentioned in 5.4.2, an ignition temperature of 343 °C was assumed in the CFD modelling of scenario 3 when evaluating timber contribution to fire growth and intensity.

The rate of charring depends on a number of parameters such as timber initial moisture content, density and temperature.[35] The external heat flux (both convective and radiative) impinging on the timber surface also plays an important role and dictates the speed at which wood is converted into char.

Butler[36] reported charring rates as a function of a wide range of radiant heat fluxes (20 kW/m^2 to 3 000 kW/m^2). The data were obtained using timber slabs having sufficient thickness to behave as a thermally-thick solid. A linear regression was provided, as shown in Formula (13):

$$\beta = 2{,}2\times10^{-2}\,\dot{q}_{rad} \tag{13}$$

where

β is the charring rate, in mm/min;

$\dot{q}_{\mathrm{rad}}$ is the radiant heat flux imposed to the timber surface, in kW/m^2.

While the range of radiant heat fluxes studied by Butler fits for the hot layer temperature predicted by the CFD modelling, the drawbacks reported would exclude it from being a suitable method for calculating charring rate in this document. It was reported by Babrauskas[37] that this linear regression is arguable given that some of the charring data was indirectly obtained from mass loss data and that the residual char density was assumed as being nil. Babrauskas[37] also mentioned that the linear regression over-estimates the charring rate when exposed to high levels of heat flux, suggesting that charring rate is not linearly proportional to the heat flux level.

Mikkola[38] evaluated the parameters affecting charring of timber, such as density, moisture content, external heat flux and oxygen concentration of the surrounding air. Among others, Spruce specimens with density of 490 kg/m^3 and a 10 % moisture content were subjected to external heat fluxes of 25 kW/m^2, 50 kW/m^2 and 75 kW/m^2 and exhibited charring rates of 0,56 mm/min, 0,80 mm/min and 1,02 mm/min, respectively. The author suggested that a linear relationship exists between the charring rate and the external heat flux in the early phase of charring (first 20 min after ignition) when the protective char layer is in its growing phase. When the char layer reaches its maximum thickness, the effect of the external heat flux is less pronounced and the charring rate decreases considerably, as observed in some room fire tests.[39] Formula (14) shows the linear relationship, which fits well with the test data.

$$\beta \sim 0{,}2\,\dot{q}_{\mathrm{e}} + 5 \tag{14}$$

where

β is the charring rate, in mm/min;

$\dot{q}_{\mathrm{e}}$ is the external heat flux imposed to the timber surface, in kW/m^2.

It is also reported by Mikkola[38] that oxygen concentration during a cone calorimeter can be taken as the normal concentration (21 %), while it is drastically reduced to 8 % - 10 % in a standard furnace test such as in ISO 834-1. A greater oxygen concentration results in an increased charring rate. White

pine exposed to an external heat flux of 40 kW/m^2 and oxygen concentrations of 21 %, 10,5 % and 0 % were reported[38] and showed that the mass loss rate decreases by 20 % and 50 % when the oxygen concentration decreased from 21 % to 10,5 % and 0 %, respectively. As such, as the fire grows within the compartment and the oxygen concentration reduces, it is expected that the charring rate will decrease.

White and Tran[40] further evaluated charring rates of various wood species exposed to constant radiant heat fluxes ranging from 15 kW/m^2 to 55 kW/m^2. Redwood (*Sequoia sempervirens*), pine (*pinus sp.*), red oak (*Quercus sp.*) and basswood (*Tilia sp.*) with average densities of 309 kg/m^3, 450 kg/m^3, 682 kg/m^3 and 408 kg/m^3, respectively, were evaluated. Specimens were conditioned to a moisture content of 8 % to 9 % prior to testing. Similarly to the linear relation suggested by Mikkola,[38] the authors found that the charring rate is proportional to the ratio of external heat flux over density (oven-dry mass and volume), according to Formula (15).

$$\beta = 5\left(\frac{\dot{q}_{\text{rad}}}{\rho}\right) + 0{,}374 \tag{15}$$

where

β is the charring rate, in mm/min;

$\dot{q}_{\text{rad}}$ is the radiant heat flux imposed to the timber surface, in kW/m^2;

ρ is the timber initial density, in kg/m^3.

Figure 25 shows the charring rate as a function of the radiant heat flux, as per Formula (13) and test data from References [38] and [40]. It also shows the predicted charring rates using White and Tran's model[40] at higher heat fluxes for pine and red oak, assuming a density of 450 kg/m^3 and 680 kg/m^3, respectively. Butler's model[36] indeed seems to over-estimate the charring rate with an increasing heat flux exposure, as reported in Reference [37]. A clear deviation between Butler's correlation and test data is observed even with exposure as low as 40 kW/m^2. Figure 26 shows a comparison between the charring rates from test data to that predicted using Formula (15), suggesting a good prediction of the charring behaviour of timber as a function of the external heat flux.

As a result, a charring model based on heat flux and density using Formula (15) is deemed reasonable and is used in the context of this example. Also, given that scenario 1 was solely used for verifying that the assumptions and parameters used in the CFD modelling are sufficiently conservative, and that scenario 2 was not considering the potential fuel contribution of the timber elements, only scenario 3 is being analyzed hereafter.

Extinction is deemed to occur when the impinging heat flux at the surface of the timber elements and the mass loss rate reduce below the thresholds cited in 5.2.2.

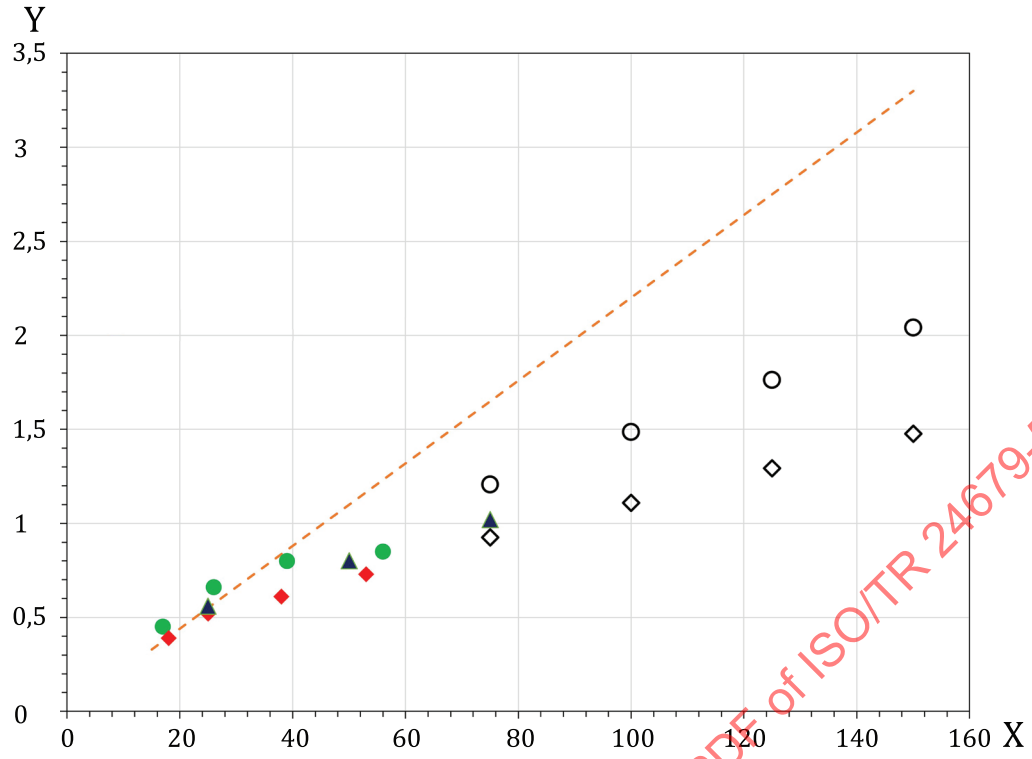

Key

X radiant heat flux (kW/m^2)

Y charring rate (mm/min)

White and Tran (1996) – test data (pine 450 kg/m^3)[40]

White and Tran (1996) – extrapolated (pine 450 kg/m^3)[40]

White and Tran (1996) – test data (oak 682 kg/m^3)[40]

White and Tran (1996) – extrapolated (oak 680 kg/m^3)[40]

Mikkola (1990) – test data (spruce 490 kg/m^3)[38]

butler (1971) – model[36]

Figure 25 — Charring rate as a function of heat flux[36],[38],[40]

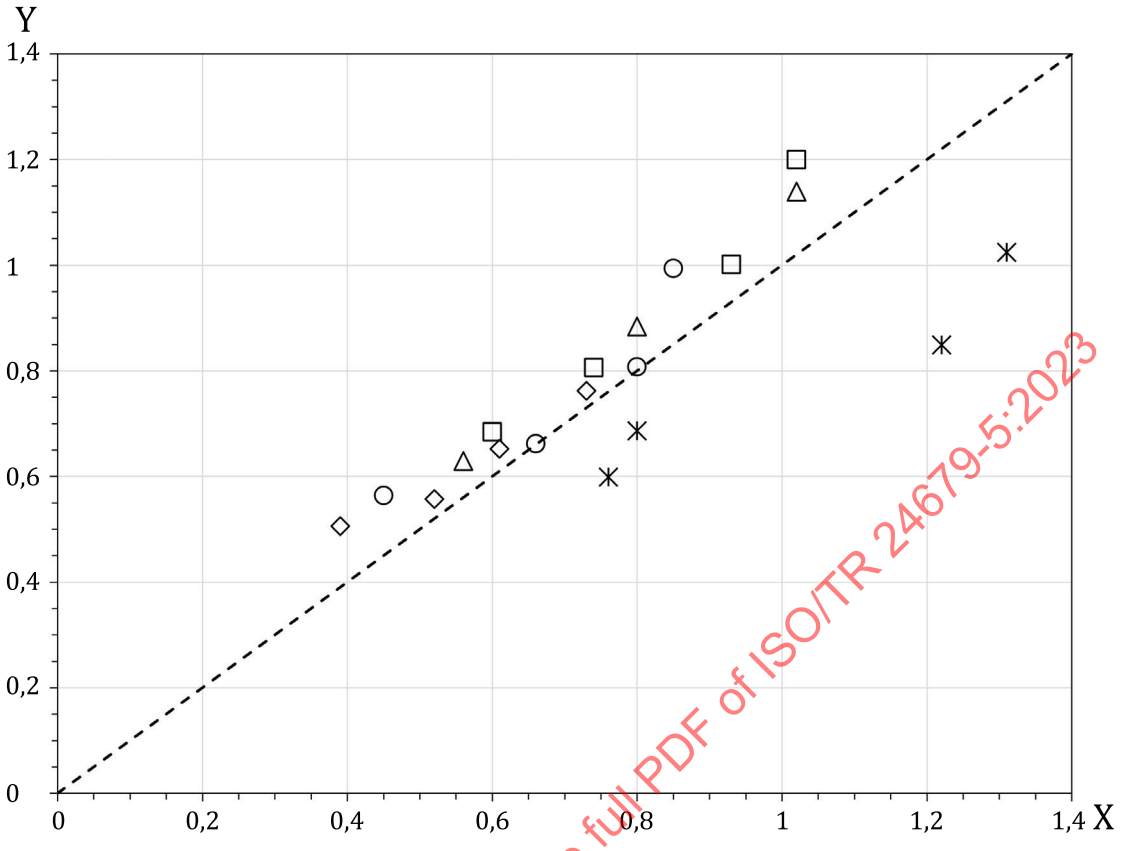

Key

X charring rate from test data (mm/min)

Y charring rate according to Formula (15) (mm/min)

○ White and Tran (1996) – pine 450 kg/m^3[40]

◇ White and Tran (1996) – oak 682 kg/m^3[40]

□ White and Tran (1996) – redwood 309 kg/m^3[40]

✳ White and Tran (1996) – basswood 408 kg/m^3[40]

△ Mikkola (1990) – spruce 490 kg/m^3[38]

Figure 26 — Charring rate as a function of heat flux — Test data compared to Formula (15)

5.5.2 Description of the thermal properties

Timber exposed to fire can ignite and contribute to fire growth and intensity. As discussed in 5.5.1, the charring rate is influenced by the impinging heat flux, which will influence the rate of heat transfer conducted into the timber element. The transient heat transfer within a solid material, such as timber, can be numerically expressed by the 3D partial differential formula that satisfies Fourier's law of heat conduction, shown by Formula (16).

$$\frac{\partial}{\partial x}\left(k_x \frac{\partial T}{\partial x}\right)+\frac{\partial}{\partial y}\left(k_y \frac{\partial T}{\partial z}\right)+\frac{\partial}{\partial z}\left(k_z \frac{\partial T}{\partial z}\right)+\dot{Q}=\rho c \frac{\partial T}{\partial t} \tag{16}$$

where

T is the temperature, in K;

$k_{x,y,z}$ are the thermal conductivities in directions x, y and z, in W·m^{-1}·K^{-1};

$\dot{Q}$ is internally generated heat by the rate of heat consumption per unit volume due to chemical reactions (pyrolysis) and the heat to evaporate water per unit volume, in W/m^3;

ρ is the density, in kg/m^3;

c is the specific heat, in $J \cdot kg^{-1} \cdot K^{-1}$;

t is the time, in s.

In an attempt to reduce computational time, mass transfer within the timber, heat of reaction due to pyrolysis and surface degradation due to cracking of the charred layer are typically ignored in numerical modelling. As such, timber thermal properties are effective values determined from test data and that implicitly consider heat and mass transfer, as reported by König and Walleij.[41] Table 9 summarizes the timber thermal properties for standard and parametric fire exposures such as those found in EN 1991-1-2[13].

Table 9 — Timber thermal properties, as presented in References [41] and [42]

Temperature °C	Thermal conductivity $W \cdot m \cdot K^{-1}$		Specific heat $kJ \cdot kg^{-1} \cdot K^{-1}$		Ratio of density to dry density	
	Parametric	Standard	Parametric	Standard	Parametric	Standard
20	0,12	0,12	1,52	1,53	1+MC	1+MC
100			1,76	1,77	1+MC	1+MC
100			13,50	13,60	1+MC	1+MC
120			13,50	13,50	1,00	1,00
120			1,64	2,12	1,00	1,00
200	0,15	0,15	2,00	2,00	1,00	1,00
200			1,28		1,00	
250				1,62		0,93
300				0,71		0,76
350	0,07	0,07	0,00	0,85	0,71	0,52
400				1,00		0,38
450			0,00		0,71	
450			0,69		0,71	
500	0,09	0,09				
600				1,40		0,28
800	0,35	0,35	0,69	1,65	0,71	0,26
1 000			0,69		0,71	
1 200	1,50	1,50	0,00	1,65	0,00	0,00

NOTE 1 Linear interpolation between values is permitted.

NOTE 2 MC = moisture content.

5.5.3 Scenario 3

5.5.3.1 Beam B1

Given the beam configuration and dimensions, only a portion of the bottom of beam B1 is left exposed and can ignite and contribute to a fire. According to the criteria detailed in 5.5.1, ignition is deemed to occur when the heat flux emitted at the beam surface exceeds 12,5 kW/m^2 and charring stops when it reduces below given heat flux and mass loss rate thresholds.

Devices for recording the surface temperature and the radiative heat flux, as detailed in Reference [24], were placed throughout the compartment, in particular underneath the mid-span of beam B1. Given

that the surface temperature and the upper layer gas temperature are almost identical, as shown in Figure 27, it is assumed that the convective heat flux has little influence and is therefore neglected when determining the surface net heat flux.

From the CFD results, ignition and charring of beam B1 located above the fire origin occurs after 4,6 min and stops after 86,3 min. At 86,3 min, the incident heat flux is 6,12 kW/m^2, the surface temperature is 306 °C and the charring rate has reduced to less than 0,45 mm/min (corresponding to a mass loss rate ≤4 g/m^2·s for a timber element of 525 kg/m^3). These are considered adequate conditions for self-extinguishment of the timber beam B1. Figure 28 illustrates the heat flux impinging the bottom of beam B1 near its mid-span as well as the oxygen concentration at that location, as predicted from the CFD modelling. The magnitude of the predicted incident heat fluxes obtained from CFD modelling are reasonable, although higher than that obtained from full-scale standard and non-standard furnace tests.[43],[44] During the rapid increase in temperature following flashover, the CFD modelling predicted a radiative heat flux of 105 kW/m^2 and 169 kW/m^2 underneath the mid-span of beam B1 when surface temperatures were 838 °C and 998 °C, respectively. A maximum value of approximately 300 kW/m^2 is predicted when the surface temperature approaches 1 230 °C. Ranger et al.[43] measured a heat flux of 100 kW/m^2 at the ceiling when the furnace temperature reached approximately 850 °C. Sultan[44] recorded a heat flux of approximately 150 kW/m^2 during standard wall and floor furnace tests when the furnace temperature reached approximately 1 000 °C.

The resulting charring rate at the bottom of beam B1 is determined using Formula (15) and the reduction effect due to oxygen concentration, as reported by Mikkola.[38] Between the period of 4,6 min and 86,3 min, a char depth of 64 mm is estimated (Figure 29), which is 4 mm above the 15,9 mm Type X gypsum board ceiling. The char progression as a function of time is consistent with the approach suggested in Reference [45]. Given the shallow portion of exposed beam below the gypsum ceiling, no side charring is assumed on beam B1 as the gypsum boards remained in place underneath beams B2 and the estimated char depth is approximately of the same position.

For structural calculations, it is common practice to subtract an additional thickness to account for the heat-affected layer underneath the char layer. For standard fire exposure, this additional thickness is linearly developing over a 20 min period, ranging from 0 mm at 0 min to 7 mm after 20 min of charring.[8],[42] The same principle is used in this study where an additional 7 mm is added to the calculated char depth of 64 mm, for a total of 71 mm. As a result, for the analytical calculation method, the reduced effective cross-section dimensions used for evaluating the load-bearing capacity of beam B1 are estimated as 265 mm (width) by 461 mm (depth).

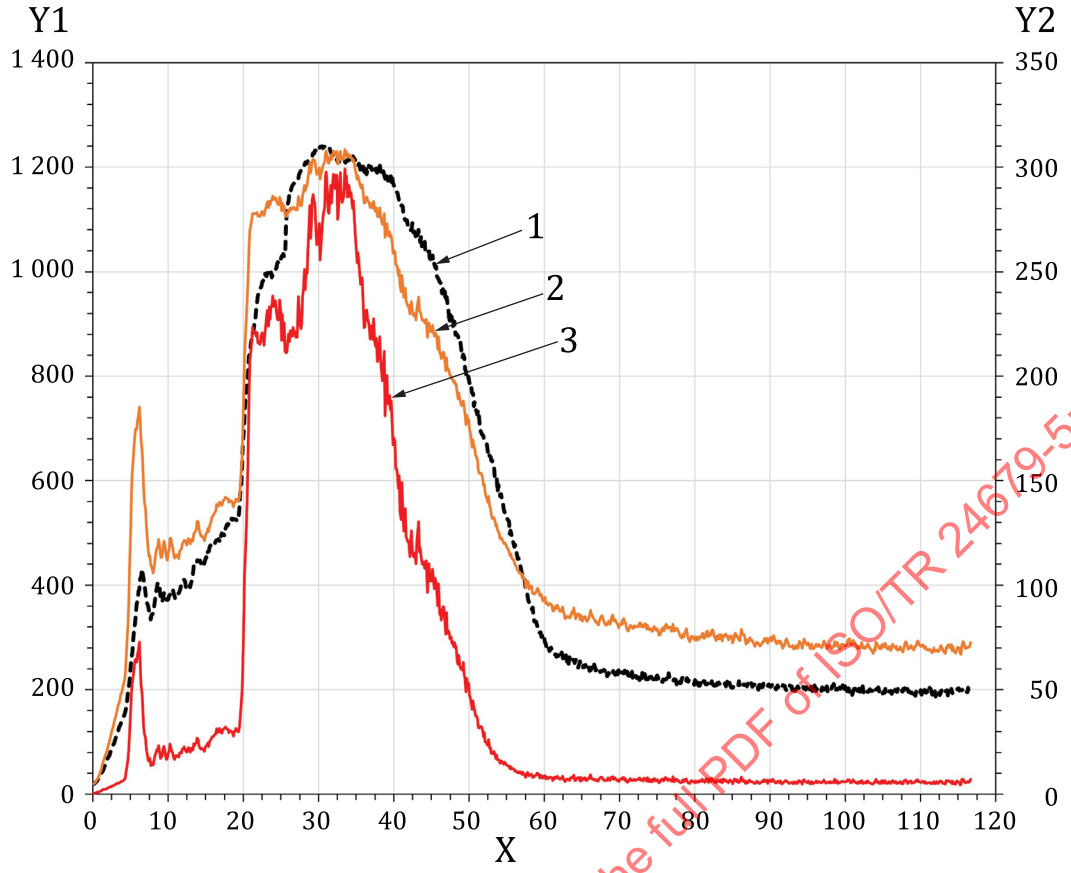

Key

X time (min)
Y1 temperature (°C)
Y2 heat flux (kW/m^2)
1 upper layer (average)
2 beam B1 – surface temperature
3 beam B1 – heat flux

Figure 27 — Radiative heat flux and surface temperature underneath beam B1 (at mid-span)

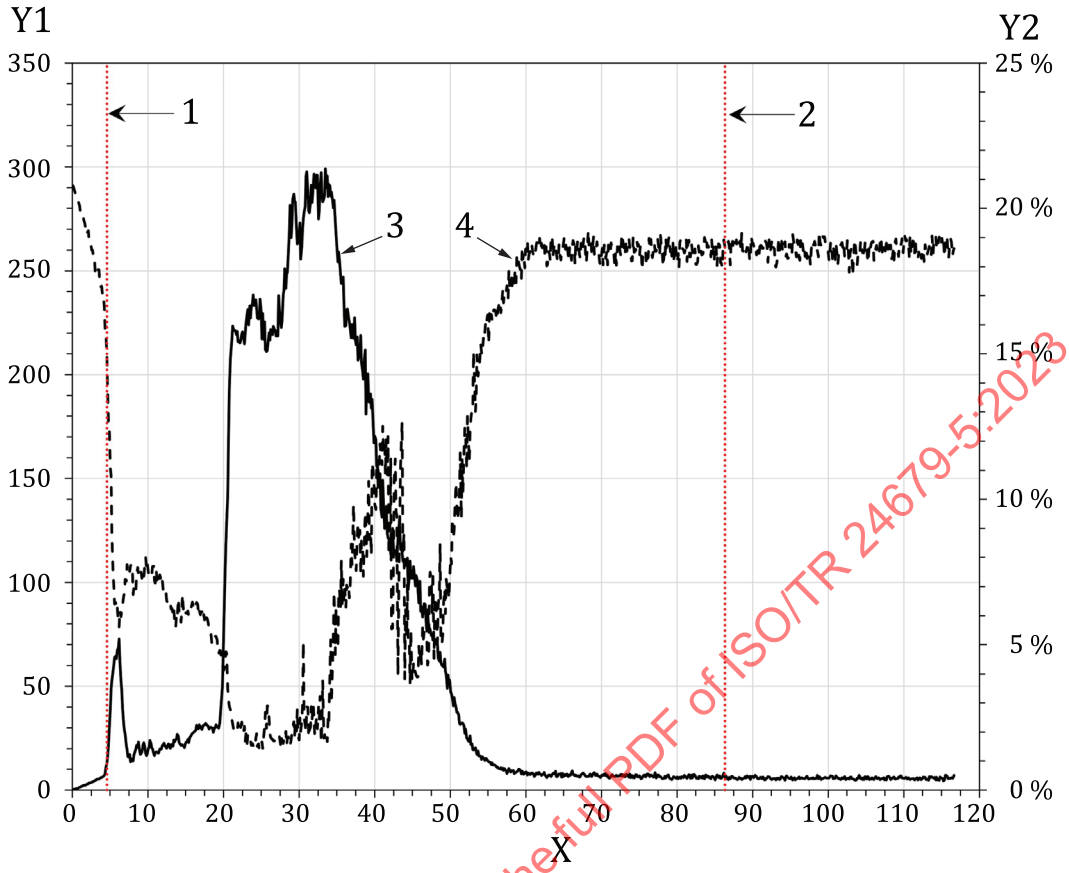

Key

X	time (min)	3	heat flux
Y1	heat flux (kW/m^2)	4	oxygen concentration
Y2	oxygen concentration (mol/mol)		
1	start of charring		
2	stop of charring		

Figure 28 — Heat flux and oxygen concentration underneath beam B1 (at mid-span)

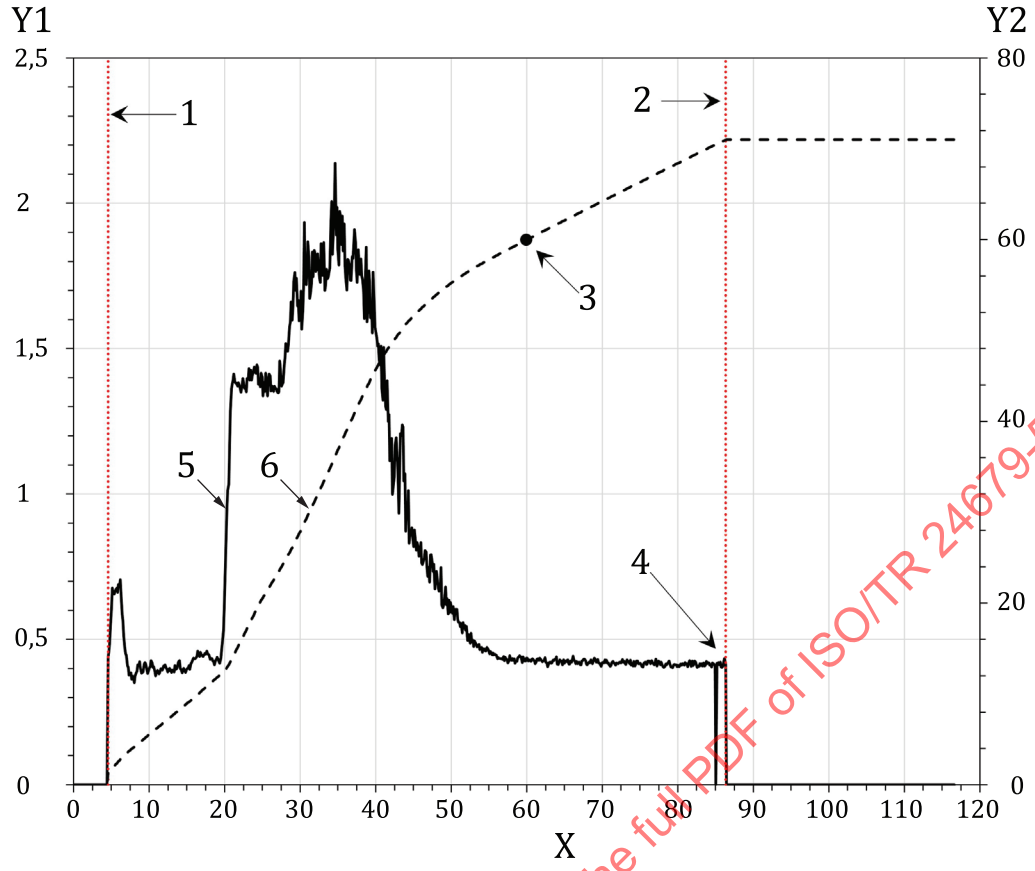

Key

X	time (min)	5	charring rate (B1 at mid-span)
Y1	charring rate (mm/min)	6	char depth (B1 at mid-span)
Y2	char depth (mm)		
1	start of charring		
2	end of charring		
3	charring after 1 h (60,0 mm)		
4	extinction when charring rate ≤ 0,45 mm/min (MLR ≤ 4 g/m^2·s)		

Figure 29 — Char depth of beam B1 as a function of charring rate

Transient heat transfer has been performed using the finite element method (FEM) from a commercially-available software package[46] and using the thermal properties for a parametric fire, as shown in Table 9. The heat flux, $\dot{q}''$, applied at the exposed surfaces of beam B1 was made using Formula (17), for explicitly considering the radiative, $\dot{q}''_{rad}$, and convective, $\dot{q}''_{conv}$, heat fluxes.

$$\dot{q}'' = \dot{q}''_{rad} + \dot{q}''_{conv} = \Phi \varepsilon_f \varepsilon_s \sigma \left(T_g^4 - T_s^4 \right) + h \left(T_g - T_s \right) \quad (17)$$

where

Φ is the view factor;

ε_f is the fire source emissivity, taken as 1,0;

ε_s is the material surface emissivity, taken as 0,80, according to Reference [42];

σ is the Stefan-Boltzman constant;

T_g is the gas temperature;

T_s is the surface temperature;

h is the convective heat transfer coefficient (taken as 35 $W \cdot m^{-2} \cdot K^{-1}$, according to Reference [13].

Figure 30 illustrates the temperature profile of beam B1. The maximum charred depth (taken at 300 °C isotherm) was reached at 49 mm from the bottom, which represents 1,3 laminations being charred. It is also slightly below the level of the gypsum ceiling. However, due to the applied heat flux to the lower portions of the sides of the beam, a light corner rounding effect is experienced, as expected, and this exceeded locally the level of the gypsum ceiling. Figure 31 illustrates the position of the char depth relative to the Type X gypsum board ceiling, as well as the residual cross-section of beam B1 using the FEM approach.

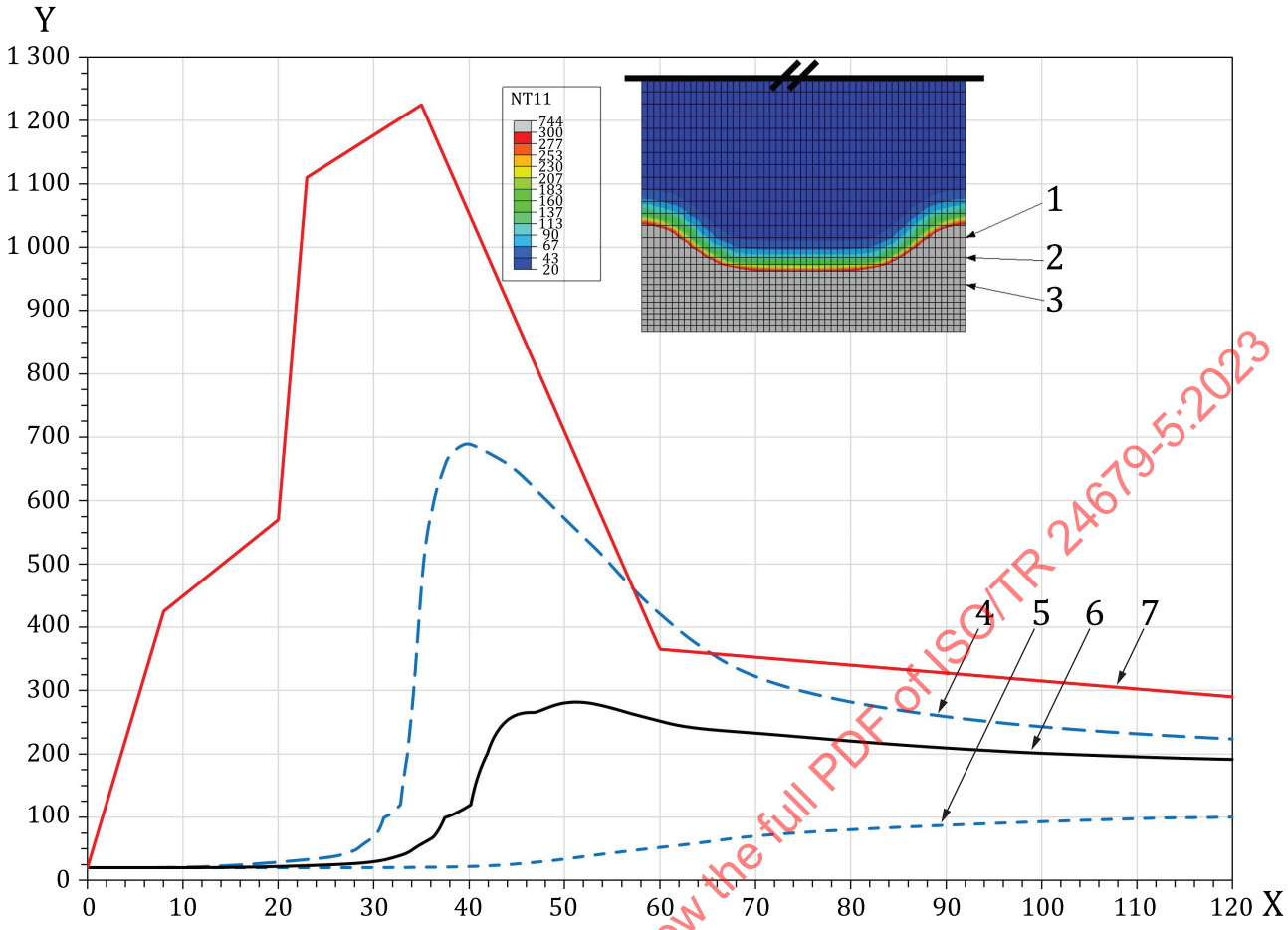

Key

X	time (min)	4	1st lamination (38 mm)
Y	temperature (°C)	5	2nd lamination (76 mm)
1	2nd lamination (76 mm)	6	49 mm depth (max. charred depth)
2	face of gypsum board (60 mm)	7	surface temperature
3	1st lamination (38 mm)		

Figure 30 — Temperature profile of beam B1: FEM approach

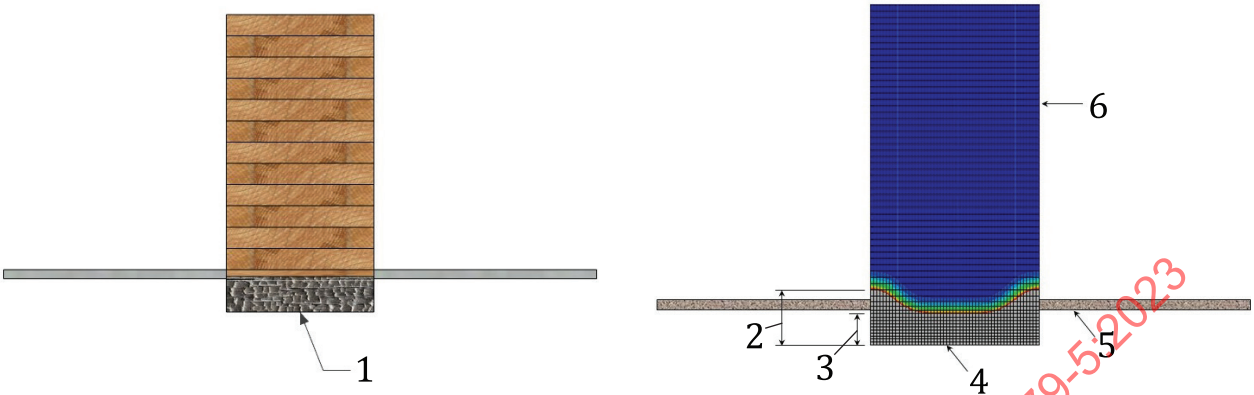

a) Analytical approach **b) FEM approach**

Key

1	64 mm char
2	86 mm
3	49 mm
4	charred layer
5	16 mm gypsum ceiling
6	beam B1 - 265 mm × 532 mm (original dimensions)

Figure 31 — Reduced cross-section due to charring: Beam B1

It is noted that the charring period between 4,6 min and 86,3 min represents the time to consume the moveable fuel load inside the office space, which is only a requirement for tall (high) buildings as determined in the applicable national prescriptive provisions. It is therefore not applicable to the 6-storey office building studied in this example. It can be rationalized that charring occurs only for 1 h, as prescriptively required for a 6-storey office building. After 1 h, the calculated char depth is estimated as 53 mm. For structural calculations, the zero-strength layer of 7 mm is to be added to the char depth and the reduced effective cross-section dimensions of beam B1 would be estimated as 265 mm (width) by 472 mm (depth). It is therefore acknowledged that evaluating the fire performance for the entire burning period of the fuel load is a conservative approach.

It is also noted that the applicable design standard prescribes a notional charring rate of 0,70 mm/min and a 7 mm zero-strength layer for glue-laminated timber exposed from 3 sides. For a 1-h fire resistance rating, a char depth of 49 mm is calculated, which is similar to those obtained from FEM and this specific fire design scenario.

5.5.3.2 Column C2

Similarly to the main beams, interior and exterior columns are partially exposed for architectural purposes. As such, only a portion of the columns can ignite and contribute to a fire. The performance criteria detailed in 5.5.3.1 for beam B1 are used for evaluating the time to ignition of column C2 and the time when charring stops.

From the CFD results, ignition and charring of column C2, supporting beam B1, occurs after 7,5 min and stops after 69,8 min. A charring rate lower than 0,45 mm/min was first reached after 57,8 min. However, at that time, the incident heat flux was 7,54 kW/m^2 and the surface temperature was 348 °C. These are considered inadequate conditions for self-extinguishment of the timber column C2. A temperature criterion of 300 °C is thus used as a criterion to determine the end of charring of column C2. This occurred at 69,8 min when the incident heat flux was 6,17 kW/m^2 (Figure 32 and Figure 33) and the charring rate was 0,43 mm/min (Figure 34), as predicted from the CFD modelling. The magnitude of

the predicted incident heat fluxes obtained from CFD modelling are reasonable, although higher than that obtained from full-scale standard and non-standard furnace tests.

The resulting charring rate at mid-height of column C2 is determined using Formula (15) and the reduction effect due to oxygen concentration, as reported by Mikkola.[38] Between the period of 7,5 min and 69,8 min, an effective char depth of 51,8 mm is estimated (Figure 34), which is before the position of the face layer of gypsum board of the exterior walls as shown in Figure 36 a). As a result, for the analytical calculation method and considering the 7 mm zero-strength layer, the reduced effective cross-section dimensions used for evaluating the load-bearing capacity of column C2 are estimated as 365 mm (width) by 283 mm (depth).

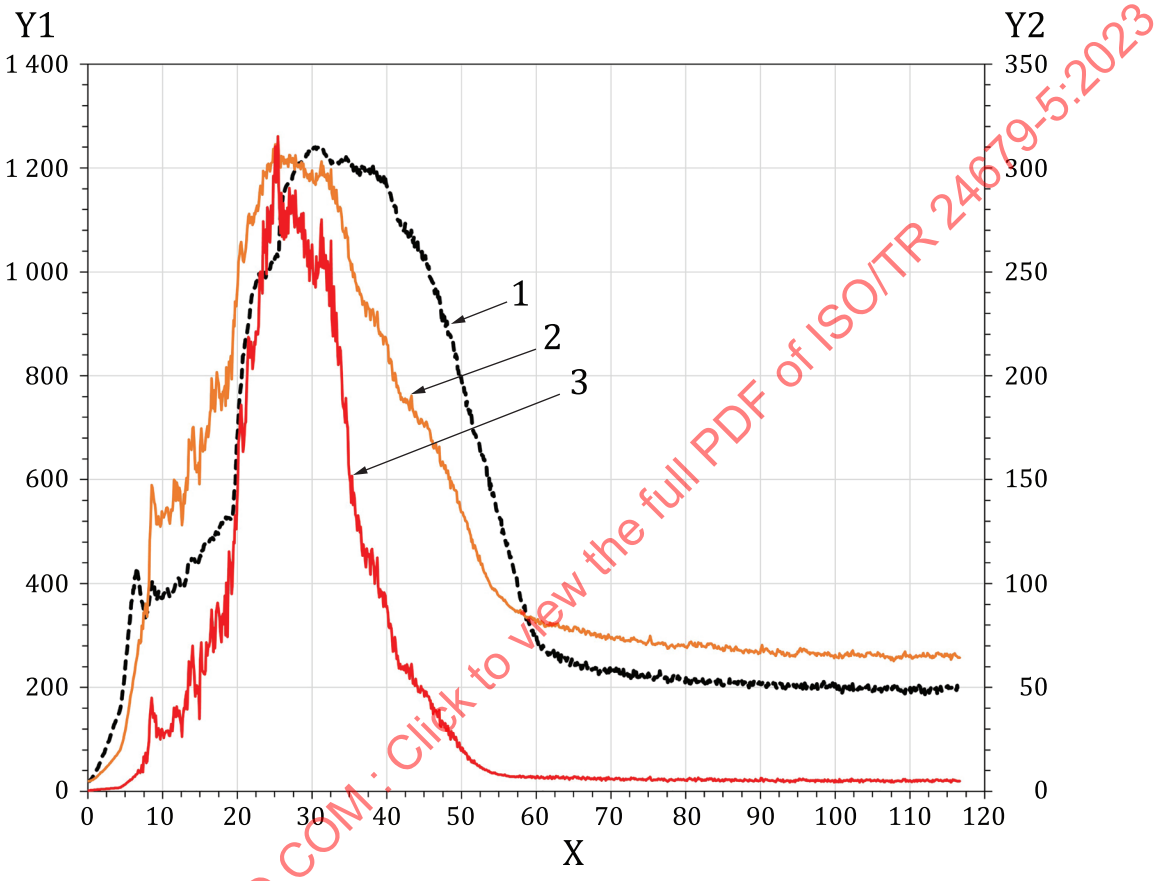

Key

X time (minutes)
Y1 temperature (°C)
Y2 heat flux (kW/m²)
1 upper layer (average)
2 column C2 – surface temperature at 1,5 m
3 column C2 – heat flux at 1,5 m

Figure 32 — Radiative heat flux and surface temperature of column C2 (at mid-height)

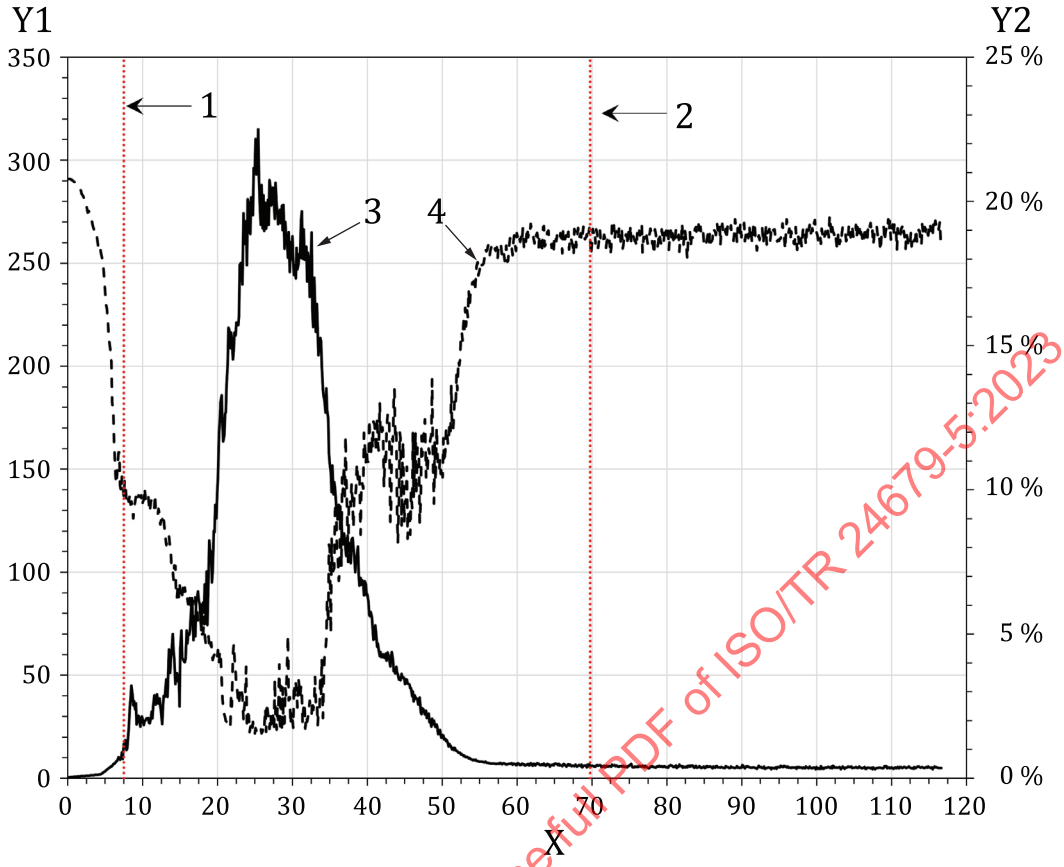

Key

X	time (minutes)	3	heat flux
Y1	heat flux (kW/m^2)	4	oxygen concentration
Y2	oxygen concentration (mol/mol)		
1	start of charring		
2	stop of charring		

Figure 33 — Heat flux and oxygen concentration of column C2 (at mid-height)

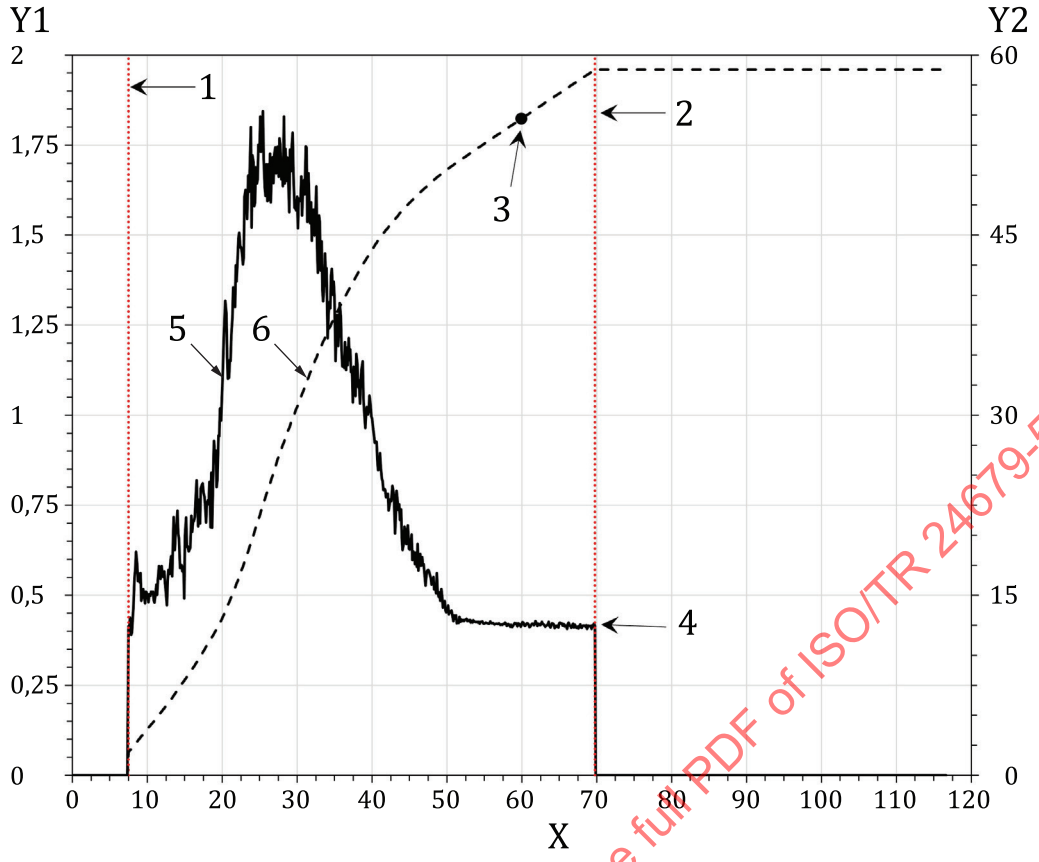

Key

X	time (minutes)	5	charring rate (C2 at 1,5 m)
Y1	charring rate (mm/min)	6	char depth (C2 at 1,5 m)
Y2	char depth (mm)		
1	start of charring		
2	stop of charring		
3	charring after 1 h (55 mm)		
4	extinction when charring rate ≤ 43 mm/min (MLR ≤ 4 g/m^2·s)		

Figure 34 — Char depth of column C2 as a function of charring rate

Similarly to beam B1, a transient heat transfer has been performed for column C2, using the thermal properties for a parametric fire (Table 9) and the surface temperature (T_s) obtained from the CFD.

Figure 35 illustrates the temperature profile of column C2. The maximum charred depth (taken at 300 °C isotherm) was reached at a depth of 43 mm from the exposed surface, which represents 1,1 laminations being charred. It is also slightly before the position of the face of the walls' gypsum board. However, due to the applied heat flux to a portion of the sides of the column, a light corner rounding effect is experienced, as expected, and this exceeded locally the level of the gypsum board. Figure 36 illustrates the residual cross-section of column C2 using the FEM approach.

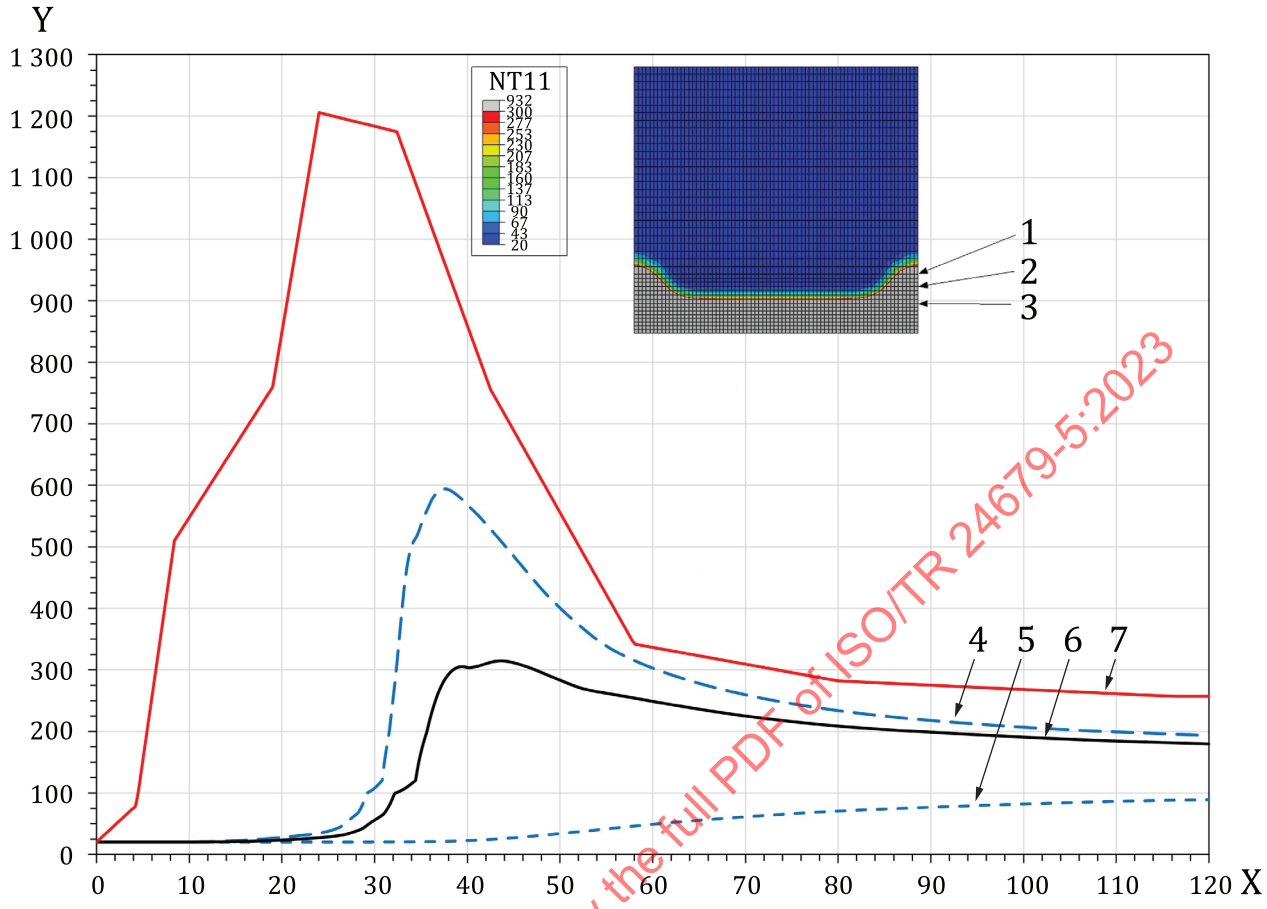

Key

X	time (min)	4	1st lamination (38 mm)
Y	temperature (°C)	5	2nd lamination (76 mm)
1	2nd lamination (76 mm)	6	at 43 mm depth (max. charred depth)
2	face of gypsum board (60 mm)	7	surface temperature
3	1st lamination (38 mm)		

Figure 35 — Temperature profile of column C2: FEM approach

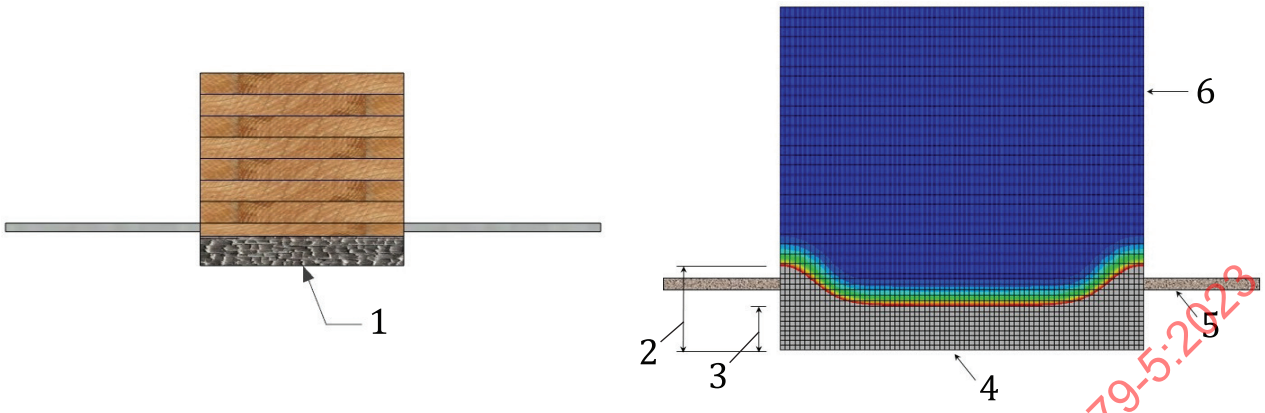

a) Analytical approach **b) FEM approach**

Key

1	52 mm char
2	86 mm
3	43 mm
4	charred layer
5	16 mm gypsum ceiling
6	column C2 - 365 mm × 342 mm (original dimensions)

Figure 36 — Reduced cross-section due to charring: column C2

As previously mentioned, designing for a full burn-out of the moveable fuel load is not applicable to a 6-storey office building which is not considered as a tall building, as determined in the applicable national prescriptive provisions. By rationalizing that charring occurs only for 1 h, a char depth of 55 mm is estimated.

Using the notional charring rate of 0,70 mm/min and a 7 mm zero-strength layer, as prescribed in CSA O86,[8] a char depth of 49 mm is calculated for a column exposed from 3 sides. This char depth of 49 mm is consistent with those obtained from FEM and this specific fire design scenario.

5.5.4 Temperature beyond the char layer

As previously mentioned, timber will experience charring when exposed to sufficient heat. Given the low thermal conductivity of char and the underlying timber beyond it, there is a steep temperature gradient within a charring timber element,[47] as presented by Formula (18). The heated zone beyond the char layer is taken as 35 mm.[8],[48] Typically, the base of the charred layer is taken at the 300 °C isotherm and there is a visual distinction between char and uncharred wood. The zone above 200 °C represents the pyrolysis zone where the timber is experiencing thermal degradation. At 100 °C, moisture is being evaporated and the timber is converted into its dry state.

$$T = T_0 + \left(T_p - T_0\right)\left(1 - \frac{x}{a}\right)^2 \tag{18}$$

where

T is the timber temperature, in °C at a position x beyond the char front, in mm;

T_0 is the timber initial temperature, in °C;

T_p is the timber temperature at which charring occurs, taken as 300 °C;

a is the thermal penetration depth for timber acting as a thermally-thick solid (taken as 35 mm).

Assuming an initial temperature T_0 of 20 °C, the 200 °C and 100 °C isotherms would be located approximately 7 mm and 16 mm beyond the char layer, respectively.

Figure 37 illustrates the temperature gradient beyond the char layer using Formula (18) and temperature data predicted by the transient heat transfer FEM modelling. The FEM predicts the thermal gradient reasonably well, which is hereafter used for evaluating the mechanical response of the timber elements.

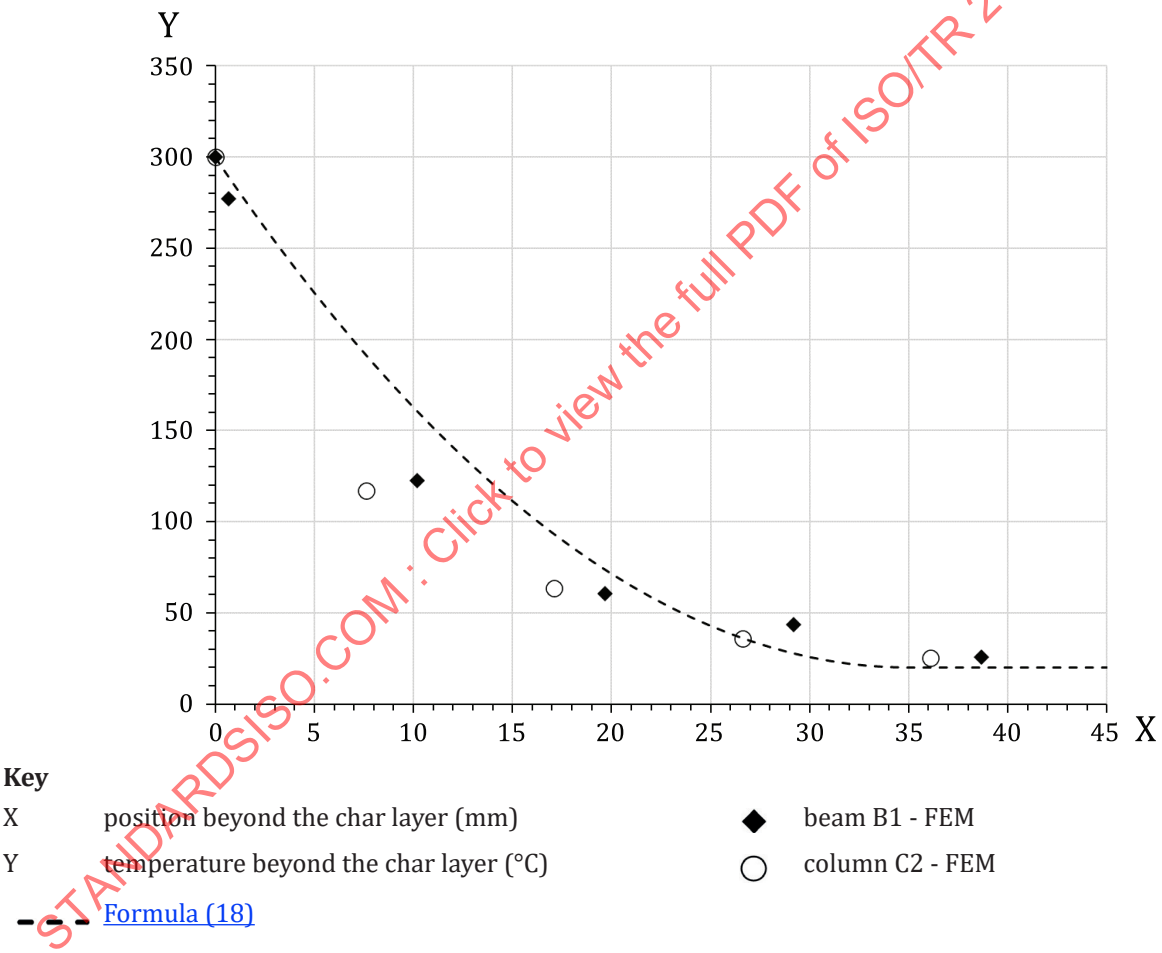

Key

X position beyond the char layer (mm)

Y temperature beyond the char layer (°C)

Formula (18)

beam B1 - FEM

column C2 - FEM

Figure 37 — Temperature gradient within a timber element

5.6 Step 6: Mechanical response of the structure

When timber is exposed to fire, pyrolysis can be initiated at the surface and charring will occur. As a result, the cross-section of a timber element reduces due to charring of the surfaces exposed to fire, which results in a change in its section properties as a function of time. As such, the applied stress is increasing with time, regardless of whether it is a bending element (beam) or axial compression element (column). Structural failure is deemed to occur when the applied stress exceeds the residual strength or excessive deflection is reached.

5.6.1 Description of the mechanical properties

Timber mechanical properties reduce when heated, as shown in Figure 38. The temperature gradient beyond the charred layer was detailed in 5.5.4.

Pyrolysis occurs at approximately 200 °C while the remaining timber converts afterwards to char at a temperature of 300 °C. As mentioned in 5.5.4, the base of the charred layer is taken at the 300 °C isotherm. The charred layer is assumed to provide no strength and stiffness to the residual cross-section.

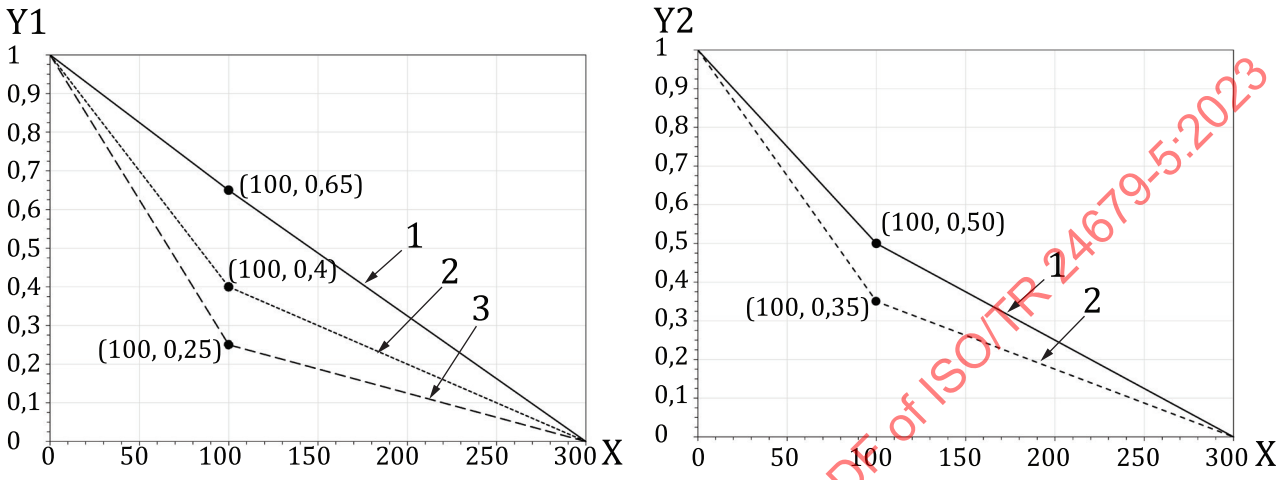

a) Relative strength

b) Relative modulus of elasticity

Key

X	temperature (°C)
Y1	relative strength
1	tension
2	compression
3	shear

Key

X	temperature (°C)
Y2	relative modulus of elasticity
1	tension
2	compression

Figure 38 — Mechanical properties of timber, as presented in EN 1995-1-2[42]

5.6.2 Scenario 3 – Beam B1

Glue-laminated timber elements, required to provide a fire-resistance rating, are manufactured following a specific layup, typically stipulated in applicable national manufacturing standards. For a fire-resistance rating of 1 h, as with this example, one core lamination is to be removed, the tension zone is moved inward, and the equivalent of one additional 38 mm thick outer lamination is added at the bottom (Figure 39). This manufacturing requirement allows for calculating the structural fire resistance of these elements using the specified strengths and modulus of elasticity values in the applicable design standard. This requirement essentially allows the additional 38 mm thick outer tension lamination to be fully charred after 1 h of standard fire exposure, without modifying the remaining layup of the residual cross-section.

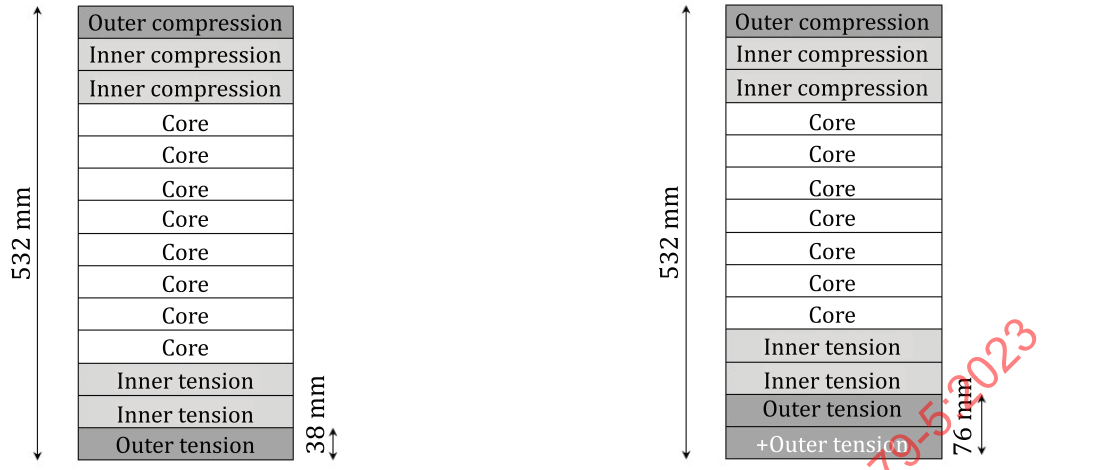

a) Unrated beam **b) Beam with 1 h fire-resistance rating**

Figure 39 — Glue-laminated timber manufacturing layup for fire-resistance

When using the analytical approach and charring rate from Formula (15), a charred depth of 64 mm is predicted, which falls in the second outer tension lamination shown in Figure 39 b). Given it is beyond the additional 38 mm outer tension lamination, an advanced evaluation of the residual strength would be required based on the actual strength and stiffness of each lamination. However, a calculation of the effective modulus of elasticity (MOE) using the actual stiffness of each lamination results in an MOE of 10 461 MPa, whereas the applicable design standard assigns an MOE of 10 300 MPa. When subtracting the 71 mm effective char depth at the bottom tension laminations, this results in an MOE of 10 419, which is still greater than the assigned value of 10 300 MPa. As such, for simplification in this example, it is assumed that the specified strengths and stiffness of a 20f-E glue-laminated timber beam are applicable to the entire cross-section (i.e. a single value of 10 300 MPa is used throughout for evaluating the mid-span deflection).

The load-bearing function of beam B1 is analytically determined using the procedures set forth in the applicable design standard and taken as the lesser of M_{r1} [Formula (19)] or M_{r2} [Formula (20)]:

$$M_{r1} = \phi(f_b K_D K_H K_{sb} K_T) S K_x K_{zbg} \quad (19)$$

$$M_{r2} = \phi(f_b K_D K_H K_{sb} K_T) S K_x K_L \quad (20)$$

where

ϕ is the resistance factor in bending, taken as 0,9;

f_b is the specified bending strength for a 20f-E Spruce glue-laminated timber, taken as 25,6 MPa;

K_D is the duration of load factor, taken as 1,15 – short-term duration, according to Reference [49];

K_H is the system factor, taken as 1,0 – no system effect;

K_{Sb} is the service condition factor for bending, taken as 1,0 – dry service conditions;

K_T is the treatment factor, taken as 1,0 – no treatment;

S is the section modulus of the cross-section;

K_x is the curvature factor, taken as 1,0 – no curvature;